Technical Report

High Ambient Temperature Heat Flux Calibration System

Arnold Engineering Development Center
Contract F40600-92-C-0011

February 11, 1993

Vatell Corporation
2001 South Main Street
Blacksburg, VA 24060

DISCLAIMER NOTICE

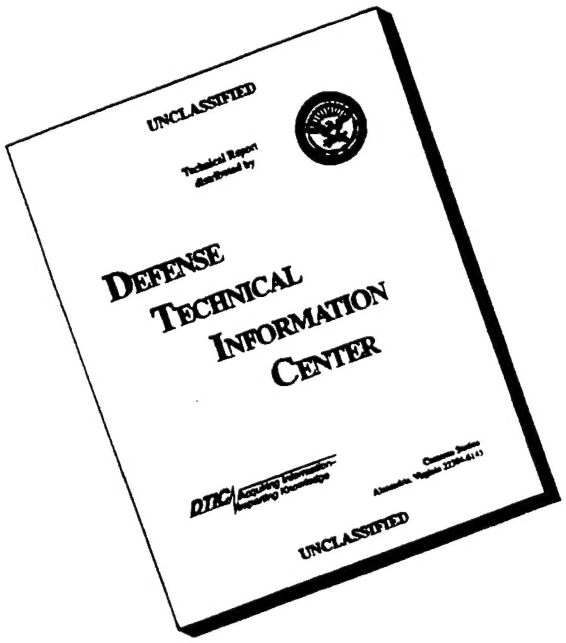

THIS DOCUMENT IS BEST QUALITY AVAILABLE. THE COPY FURNISHED TO DTIC CONTAINED A SIGNIFICANT NUMBER OF PAGES WHICH DO NOT REPRODUCE LEGIBLY.

Table of Contents

Summary

In this contract Vatell Corporation explored source and temperature control concepts for high ambient temperature heat flux calibration. Three alternative calibration methods were studied: (1) concentrated high intensity light radiation, (2) heated graphite block radiation and (3) convection. Neither the graphite block method nor the convection method could match the temperature and heat flux range of the concentrated high intensity light method, which was selected for development of a preliminary system design. The best currently available equipment and technology for radiation calibration were combined in the design, to achieve calibrations at up to 815°C with heat fluxes of up to 1136 W/cm². A tentative list of equipment, including costs, was compiled for the system.

Methods for separate measurements of convective and radiative flux at a surface were explored analytically. An experimental method was proposed for possible evaluation and test. The method uses two Heat Flux Microsensors with different emissivities on a single probe or surface, and enables computation of the relationship between emissivity and heat flux at the surface.

A new type of heat flux standard was proposed which would be referenced to electrical measurements instead of radiation. If this device could be demonstrated and proven, it might ultimately replace the slug calorimeter as the standard sensor in heat flux calibrators.

Task 1 - High Intensity Light Calibration System Design

In this task we explored alternatives for a heat flux sensor calibration system which would employ the same type of energy source as the system now in use at AEDC, but would allow the temperature of the sensor to be controlled up to 815°C. A critical issue in the design was whether a vacuum enclosure must be provided for the sensor being calibrated. We weighed the pros and cons of the vacuum enclosure, and decided to include it. However, it will be possible to operate the system without evacuating the chamber, with some reduction in accuracy and a small margin of additional convenience. The importance of the vacuum environment to calibration accuracy, and to operating convenience, can easily be determined during initial use of the system. Then the user can decide when and under what circumstances to evacuate the chamber.

An absolute need for the vacuum environment will exist if the user intends to calibrate sensors at high temperatures and low heat fluxes. This is because the convective losses of the sensor in air at high temperatures would be variable and indeterminate. If only high heat flux calibrations will be performed at elevated temperatures, the vacuum environment is unnecessary.

Another important factor in deciding whether to provide a vacuum chamber is the calibration accuracy objective. If calibrations are to be performed to 5% of full scale (and only at high heat fluxes), the vacuum environment is probably not necessary. If improved accuracy is sought, say 2% of full scale, and low heat fluxes are important, then the vacuum chamber is certainly required.

The most general solution, and the one which has the greatest range and capability for precision, is an evacuated system. To meet possible objections about user inconvenience or other limitations, we have designed the system for full access to all components during loading and unloading, and for almost totally automated calibration cycles. These design features will maximize convenience of use and minimize the labor required for calibrations under vacuum. Appendix A is a list of the equipment proposed, including prices. Appendix B is a description of the design, fabrication and delivery process which is planned for a Phase II continuation of this project.

Controlled Temperature and Environment Chamber

A simple system could be designed to heat sensors up to 815°C if the objective was just to elevate their temperatures. This application requires, instead, that sensors be subjected to heat fluxes of various magnitudes while at elevated temperatures. Both the incident heat flux and the losses of heat to the environment must be known to achieve accurate calibrations. For this reason we have designed a closed chamber to house and insulate all components whose temperature is controlled. The chamber reduces the paths and modes of heat loss by the sensors. Addition of a vacuum environment in the chamber confines losses from the heated sensors to only two modes of heat transfer, conduction and radiation, both of which can be modelled and analyzed.

The vacuum chamber eliminates unpredictable heat losses caused by forced convection. Opening and closing of doors, operation of building HVAC and movement of personnel in close proximity to the equipment would produce forced convective losses that cannot be predicted. A heated surface in a chamber at atmospheric or greater pressure is also subject to natural convection. We estimated losses by natural convection for the sensors in the heated calibration apparatus. The estimates were based on calculated losses from a heated cylinder at the same temperature. Different pressures were assumed to predict the level of vacuum which would be necessary to make the losses insignificant. The calculations use the Grashof number, Gr_L. This number indicates the ratio of the buoyancy force to the viscous force acting on the fluid, where a strong buoyancy force predicts energy transfer by natural convection. The Nusselt number is also a factor but must be corrected using Kn.

The equation and constants are:

ΔT = 1000°C
L = 0.05 m
β = 1/300
A = 118 cm²

$$Gr_L = \frac{g\,B\,L^3\,\Delta T\,\rho^2}{\mu^2}$$

$$Nu = 0.372\,(Gr_L Pr)^{0.25} = \frac{hL}{k}$$

$$q''_{tot} = h\,\Delta T$$

$$\rho = \frac{P}{R\,T}$$

The estimates were as follows:

Pressure	Kn	Heat Loss (watts)
101 kPa	0	190
1 Kpa	10^{-4}	15
133.32 Pa	8×10^{-4}	3.1
13.33 Pa	8×10^{-3}	0.75
1.33 Pa	0.08	0.17
0.133 Pa	0.81	0.022

(Note: Kn was determined from figure A1 in Progress Report #4)

These results show that free convection is reduced to an acceptable level when the pressure is less than 13 Pa. This level of vacuum is easily achieved using a rotary vane pump and can be reached in about three minutes in the proposed chamber. Since the vacuum is not very high, it is a simple matter to bring the chamber back up to atmosphere.

Natural convective losses would make a substantial contribution to measurement uncertainty when the sensor temperature is high and the incident heat flux is low. This is a unique combination of circumstances which may not be of immediate interest to the user. The calculations above show that natural convective losses can be important at the extremes of the system requirements. It is up to the user to evaluate whether the measurement uncertainty caused by

natural convection at intermediate levels of heat flux is acceptable or not. We decided that a truly accurate calibration system would require control of all error sources which might adversely impact system accuracy with any combination of system conditions. Since natural convection is a difficult loss to quantify, it was important to minimize and control it. Our design reduces it to a negligible loss, as illustrated in the table above.

Most users, especially those who are familiar with conventional high vacuum systems, will feel that the equipment required for a vacuum system is large, fragile and complex. They may also fear that placing system parts in a vacuum environment would make them inaccessible and that the process of removing and replacing them would be time consuming. The design we propose here avoids these problems. The entire sensor mounting assembly with its connections can be completely removed from the chamber. The time required to achieve a working vacuum is quite short, allowing a quick return to testing conditions after sensor replacement or adjustment.

The proposed system uses high vacuum technology even though it operates at a low level of vacuum. Costs typically attributed to these systems will be greatly reduced by custom design. The stainless steel chamber construction with ultra high vacuum seals is necessary to meet the temperature requirements of the contract and incidentally results in a more durable and reliable system. The design will allow operation to be extended beyond the requirements of the original proposal. We have tried to build in versatility which will allow the user to define the limits of system usage, to evaluate other characteristics of heat flux sensors, and to operate the system in a manner consistent with the accuracy objective.

There is an additional advantage to the class of hardware chosen for the system. We have found that alignment of sensors relative to the source is often critical. The proposed system is rigidly constructed in a manner that will hold sensor alignment through multiple mounting cycles. The sensor exchange system which centers sensors in the test position is enclosed within the chamber and is therefore protected from accidental damage while it is not in use. While initial accuracy of the system is important, the ability to retain this accuracy is of equal importance.

Chamber Design

The Phase I solicitation requires that an area of 1 inch diameter must be irradiated uniformly for calibrations with up to 1000 Btu/ft^2-sec of heat flux. Only one sensor will be irradiated at a time because it would be prohibitively costly to irradiate two or more sensors at a time. The system will be designed to center either a standard sensor or a sensor for calibration in the 1" diameter area. All optics, shutters, windows and source components will be in fixed positions. The size of the source and the

accuracy required for alignment of the optics require that the sensors be moved.

In a preliminary design we proposed to move the chamber relative to the source in order to reduce the complexity of the fixtures within the vacuum chamber. This required either two viewports or one very large viewport. The design raised concerns about errors which would result from differences in the transmissivity of the two viewports or across a given viewport. It was also felt that thermal stresses on a large viewport might cause damage or unknown variations in its optical properties.

After we decided that the sensors would be positioned in front of a single irradiation port within the vacuum chamber, we explored designs for linear translation under computer control. A number of problems surfaced during the design process. To provide the necessary spacing between the sensors for thermal isolation, the linear stage would have to be quite long. To allow free travel of the sensor holder within the chamber, instrumentation leads, power leads, and cooling lines would have to be long enough for minimum flexing. When we added provisions for open user access to mount and demount sensors, the physical size of the system became unreasonable. A long rail system would be required at the end of the chamber so that sensors could be moved to a position totally outside the chamber. This system turned out to be quite large, as shown in Figure 1.

Since the method chosen for sensor exchange seemed to be the dominant influence on the chamber size, we decided to explore a more compact sensor exchange method. At this point it also became clear that the source and its optics would be quite large, so the orientation of the chamber became important. In the original design the source was mounted above the chamber. This arrangement would be so tall that access to some components of the system would be difficult. Also, the stage on which sensors would be mounted for calibration would be moved in and out of the chamber vertically. A motor drive would be needed to handle its weight and safely control its motion. We decided to change the orientation of the system axis to horizontal.

Sensor Support and Exchange Mechanism

In the final design, Figures 2 and 3, the mechanism that exchanges the sensors in front of the source was changed to a rotary swing arm. This provides enough travel for sensor exchange without much flexing of wires and cooling lines. The swing arm design achieves the same physical separation of the sensors as the linear system, and uses the space within a round chamber more efficiently. This allows a reduction in the overall chamber size. It also eliminates a difficulty of the earlier design in which the irradiation port was on the side of the cylindrical chamber. The final design has the irradiation port in one of the end caps. This became

necessary, anyway, when it was found that the irradiation port would have to be quite large, and would probably be fabricated by an outside supplier.

The chamber is cylindrical with two flanged end caps. One end cap is bolted on and contains the irradiation port, while the other is removable and contains sensor mounting stages and instrumentation. The chamber has two side ports which may be used for visual inspection during calibrations. A light source will illuminate the inside of the chamber through one, while the user may look through the other with the aid of a mirror. Tabs are welded to the chamber to attach it to the system baseplate. All ports will have copper gasketed high vacuum seals, except for the removable end cap which is opened to mount and demount the sensors. This end cap will have a rubber seal for easy removal and replacement. The other ports may reach high temperatures which rubber seals could not withstand. The user should never need to remove any of the other ports.

The removable end cap which provides access to the sensors and their mounting stages will not have any clamping or fastening hardware. The advantage of the rubber seal is that the end cap can be manually held against it as the vacuum pump is turned on, and the force created by the vacuum will then hold the end cap in place. This will reduce the time and effort involved in beginning tests after changing or adjusting sensors. The removable end cap will be mounted on a bracket fitted with bearing blocks which ride on rails. These will support it through its free travel. Since the chamber is positioned on its side, the translating mechanism for the removal of this end cap can be manually operated. The rails will be fixed to the chamber supports for accurate alignment, and are long enough for the end cap to be pulled back so the sensors are completely clear of the chamber.

The removable end cap is fitted with a rotary motion feed-through, an electrical feed-through for the heaters, two feed-throughs for cooling air, and two instrumentation feed-throughs to accommodate 16 inputs or outputs to the evacuated space. The feed-throughs for heater power will handle considerable current, and are separated from the instrumentation feed-throughs to minimize noise pickup.

The air cooling feed-throughs are included for an optional cooling function. This function would not be used to control the sensor holder temperature, but only for rapid cooling between tests or at the end of a series of tests. The latter would be a convenience to the user, who would not be able to handle the sensors until they have reached a temperature close to ambient. During the commissioning of the system we will find out if rapid cooling has sufficient advantages to justify the extra cost. This feature might be useful when the set-point temperature for a test is equal to or lower than that of the preceding one. This would allow more rapid cycling of tests, particularly at high flux levels. Air cooling would reduce the temperature of the sensor holder more

quickly than just allowing it to cool by radiation loss. Addition of the capability for cooling may add to system versatility, and will certainly reduce test durations.

With the rotary swing arm sensor exchange design there is only a small change in length of the cooling lines as the sensors are positioned. This motion can be accommodated by incorporating short lengths of flexible stainless steel tubing. Other flexible tubing, such as plastic, would not withstand the temperatures. The location of the flexible tubing is shown in the system assembly, Figure 2.

The rotary motion feed-through is turned to center one or the other sensor in front of the irradiation port, or to profile the heat flux along an arc which crosses the port. Its shaft will be driven from the outside of the chamber by a computer controlled stepping motor. Inside the chamber the shaft will be supported by a second bearing in the opposite end cap of the chamber when the removable end cap is in place against its rubber gasket. This will provide sufficiently rigid support for precise and repeatable sensor location. Mounted on the shaft will be the swing arm, sufficiently rigid to prevent significant deflection in any of its positions. The sensor heater stages will be mounted on the end of this swing arm.

The sensor heater stages will be attached to the swing arm by thin walled support cylinders. These will be stiffer than the two or three small diameter standoffs which were used in an earlier design. The heater power wires will be fixed to the outside of the support cylinders. All other wiring will be located on the inside of these cylinders. All permanent leads (not those to the sensors) will be fixed to the inner walls of the cylinders. The sensor wires will pass through the cylinders, but will not be fixed to it. This should make it easier for these leads to be installed and removed. When a sensor is exchanged, the leads will be fed through the hole in the heater stage, through the cylinder, through a hole in the swing arm and then over to the instrumentation feed-throughs. The insulation on the lead wires for the sensors must be able to withstand the maximum temperature of the sensor tests. The inside of the heater stage and the tube will reach the same temperature as the sensor during the test. To prevent the removable end cap from overheating, a mirrored shield will be positioned between the two heater stages and the inside of the end cap. If it is found that the end cap temperature still exceeds 250°C, air cooling lines can be brazed to the outside of the flange next to the seal.

Heater Stage Design

A standard heat flux sensor mounting stage has been designed and its thermal properties analyzed by finite element methods. This stage will be used to mount the five different types of heat flux

sensors to be calibrated within the vacuum chamber. The sensors which will be accommodated are the (1) Schmidt-Boelter, (2) Gardon, (3) Null-Point Calorimeter, (4) Coaxial Surface Thermocouple, and the (5) Vatell Heat Flux Microsensor. The stage consists of a sleeve (Figure 4), and a universal plug (Detail "A", Figure 4). In an earlier design the sleeve was made from nickel, which has high thermal conductivity and wide temperature tolerance. Electrical insulation of the heater wires from a metal sleeve would be quite complex because of the requirement for very good heat transfer. We initially selected Nextel, a cloth-type insulation, for the heater filament wire. There was some concern about the heat transfer through this insulation, and possible electrical leakage between the filament and the metal sleeve. Since the sleeve is metal, it must be grounded to minimize electrical noise.

Another type of insulation which could be used is a ceramic bead type. With this, the effective filament diameter would be increased and the number of turns reduced. A third option is to plasma spray the nickel sleeve, coating the inside of the helical groove. This requires special fixturing for plasma spraying and would need to be explored further to find out if a uniform coating can be achieved. A fourth alternative would be to fabricate the sleeve out of a boron nitride, an electrical insulator with high thermal conductivity. This is the alternative we have selected.

To make the heat flux sensor stage, the outer diameter of a cylinder of boron nitride will be machined with a helical groove. A heater wire wound in this groove will be electrically isolated but in good thermal contact with the cylinder. We performed the following analysis to determine the length of the heater wire and its performance;

Parameters

V_{fixed}= 115 V (outlet voltage)
I_{max}= 20 amps (current drawn)
R_{min}= 5.75 Ω (wire resistance)
P_{max}= 2300 watts (power dissipated)
ρ_e= 0.441 E-6 Ω•m (Constantan)
d = 5.1054 E-4 m = .0201 in. (wire diameter)
A = 2.047 E-7 m^2 = 3.173 E-4 in^2 (wire cross-sectional area)

Using,

$$R=\rho_e l/A$$

l_{min}=(length of wire)=2.67 m = 105 in

This length was used to determine the height of the boron nitride sleeve. The wire is 0.0201 inches in diameter. The heater sleeve outside diameter is 1.5 inches. This requires 23 wraps around the sleeve with a sleeve height of 0.9 inches to achieve the required

length, l_{min}.

The above design appears to be reasonable, but these are not necessarily the final dimensions and parameters. We used finite element analysis to estimate the heat-up times with the proposed power input. The finite element model is a 1 radian pie-shaped slice of the axisymmetric sleeve and plug (Figure 5).

The finite element model embodies some assumptions that will not be true in the actual apparatus. First, it is assumed that there are no thermal losses. All power put into the model is stored within it. Second, perfect thermal contact is assumed between the heater wire winding and the boron nitride sleeve. Third, perfect thermal contact is assumed between the sleeve and the instrumented plug. In the actual stage there will be some losses from radiation to the chamber walls and some heat conducted to the support. Convective losses will be negligible in the vacuum environment. The thermal resistance between the heater winding and the sleeve will not be negligible. There will also be a finite thermal resistance between the heater sleeve and plug.

Of the five heat flux sensors this apparatus is designed to accommodate, four have negligible thermal mass compared to the sleeve and plug. The finite element model of the sleeve and plug alone adequately predicts heat-up times. When the Heat Flux Microsensor is tested, it replaces the nickel plug. The thermal properties and geometry of the microsensor substrate are significantly different from those of the nickel plug. For this reason, the model for microsensor heat-up times is different from the others. The results of the analysis are shown in Figures 6-9.

The heat-up times found in the analysis are reasonable for a calibration system which will be used in this manner. Considering that the actual losses and thermal resistances of the apparatus are unknown, it would not be unduly conservative to increase these times by a factor of ten. Even these increased times are acceptable in terms of testing convenience.

The heater stage for the sensor being calibrated will be raised to temperatures as high as 815°C. The radiation losses at this temperature will be substantial. They were calculated using the following equation:

$$q = f\epsilon\sigma A\,(T_1^4 - T_2^4)$$

Assuming f = ϵ = 1, and dividing by the exposed area of the heater stage, the heat flux loss by radiation would be 7.92 W/cm². This is not enough to affect the calibration directly, but will heat the walls of the vacuum chamber. More important, it could affect the thermal environment and temperature of the standard sensor. A radiation shield will be necessary around one or both of the heater

stages. The shield(s) will be made from quartz, 3 inches inside diameter, 3 inches long with a 1/16 inch wall thickness. The tubes will be coated on the inside with gold and magnesium fluoride by EMF Corporation. Magnesium fluoride provides abrasion resistance. The gold has a reflectivity of 96% in the infrared radiation range, and will reflect most of the radiated energy back to the stage. The shields will be attached to the tube which supports the heater stage as shown in Figure 10.

The mounting stage for the standard sensor will normally be heated just enough to provide accurate temperature control in the presence of thermal loads from the other heater stage and the chamber environment. This stage will have the capacity to reach 815°C, however, so it could also be used for the full range of tests.

Proposed Radiation Source

The following is a description of the radiative heating source proposed for use with our system by Spectrolab Inc. This company has built optical systems for NASA in which a lens was used as the window into a vacuum chamber. Originally Spectrolab proposed an "off the shelf" steady-state heating system using a water-cooled 20 to 30 Kw xenon high pressure short arc lamp. This system is their X-200 solar simulator (see Appendix C), which Spectrolab produces in quantity. The spectral distribution of a typical 20 Kw xenon arc lamp is shown in Figure 11. Most of the radiation falls in the visible and infrared. These wavelengths are readily absorbed by many available coatings. After some analysis they decided a pulsed system would better meet the requirements at reduced cost.

The X-200 normally uses multi-element optics to integrate the beam for very good uniformity across a large test plane. The heat flux levels attained with these optics are well below the requirements of this contract. To achieve the heat flux objective these optics would be replaced by a 22 inch aconic collector in the source module. This would be combined with a two element concentration lens assembly as shown in figure 12. The second lens would also serve as the window into the vacuum chamber. The major modules of the X-200 assembly are:

Source Module (houses XE water cooled source)
Source Box (supports source module and optics)
LC52 Power Supply (provides up to 650 amps stable dc power)
Water Cooled Cables (provides coolant to X-200)
Water Conditioning Unit (provides high pressure DI water)
Concentration Vacuum Window Lens Assembly
Module Controller (provides required controls and safety features)
Auxiliary Shutter (located in source box)

Spectrolab engineering has investigated the task of combining the 22 inch aconic collector with a concentration lens to distribute

lamp radiant energy uniformly over a one inch diameter sensor test plane. They concluded that while a single lens could be made to work, it would be better to use a doublet. Peak irradiance levels far exceeding the proposed requirements are possible but achieving uniformity over the one inch diameter is difficult.

The first lens of the doublet will be a plano convex lens with its flat side towards the sensor. The second lens will be a plano concave lens with the concave surface facing the sensor. This lens would also serve as the vacuum chamber window.

Irradiance levels have been estimated using several different methods of analysis. One approach utilized the source radiance characteristics and predicts the average irradiance over the one inch diameter sensor plane based upon estimates of the effective useful arc radiance, optical attenuation, and the total solid angle of irradiance. A second approach estimates the efficiency factors associated with transferring radiation to the one inch area. These efficiency factors include: power conversion, obstruction factor, flux collection factor, reflectance of the collector and arc utilization factor, which is a function of the arc magnification as viewed from various angular zones. For this design it is defined as the radiation that strikes the one inch diameter area compared to the total radiation transmitted through the concentration lens, expressed as a percentage.

A third approach uses existing irradiance data at a test plane with 20 Kw operation using the 22 inch collector. For the single lens concept, optical rays from both the anode and cathode tip of the arc have been traced through the optical components to the target plane, see figure 13. Their intercepts on this plane can be used to estimate the resulting power distribution at the test plane. Knowledge of the total power incident on the lens assembly and the power distribution derived from the ray tracing can lead to reasonable performance predictions.

These three "proof of concept" approaches have only been applied in a rough order of magnitude type appraisal. However the estimates were conservative and they all indicate that the desired irradiance level can be achieved.

The peak irradiance achievable on the optical axis is constrained by the following:

A) The effective radiance of the source, viewed through the optics.
B) The optical attenuation of the radiance by the optics.
C) The geometrical angles associated with the solid angle of irradiance.

The irradiance incident on a point on the test plane can be expressed by the following equation;

$$E(MAX) = \pi * L * K * (\sin^2 \phi/2)$$

Where: L = The effective radiance of that part of the arc in use
K = The attenuation factor caused by the optics to attenuate the effective arc radiance
$\phi/2$ = Half angle of the solid cone of irradiance

For the proposed system K is equal to approximately .72, made up of the product of two lens transmission factors and one collector reflectance factor. $\phi/2$ will be no more than 45° although the initial design showed a slightly faster concentrator system. The following table shows various test plane irradiance levels resulting from various effective radiance values. This is a center line maximum irradiance limitation based upon the arc radiance. The arc is not uniform in radiance, in fact, it is very non-uniform. The lower the effective radiance requirements, the larger the portion of the arc which can be used. In other words, there is a tradeoff between uniformity and total irradiance.

ARC RADIANCE L (W/cm^2-STER)	IRRADIANCE CENTER LINE (W/cm^2)
6000	6780
5000	5655
4000	4524
3000	3393
2000	2262
1000	1131

The above radiometric evaluation indicates that there is no radiance restraint regarding center line irradiation. Off axis positions on the target plane may not see the arc in its full field of view. Hence the average effective radiance would be significantly reduced.

The following are efficiency factors used in the initial evaluation of test plane performance:

Power conversion	0.55	
Obstruction Factor	0.97	
Flux Collection	0.73	
Collector Reflectance	0.85	
Lens Transmittance	0.85	(Two lens)
Test Plane Arc Utilization	0.30	(Soft number without further study)
Total Efficiency	0.084	

Using this efficiency and assuming 20 Kw electrical input power we get:

Power at Test Plane (.084)(20,000) = 1680 Watts within one inch diameter

Test Plane Irradiance = 332 W/cm^2

This is less than 30% of the desired irradiance level. Operation at 25 Kw would increase the irradiance level to approximately 415 W/cm^2. To achieve the desired 1140 W/cm^2 will require either of the following:

1) Increase the arc utilization factor from .3 to about .824 with operation at 25 Kw or,
2) Operate at an input power level of at least 69 Kw, assuming the .3 arc utilization factor cannot be improved.

Conclusions: Achievement of a .824 arc utilization factor is probably not possible. However the input power can probably be raised to 70 Kw or above if the time spent at that power is limited. Lamp overdrive is restricted only by the lamp thermal envelope. Based on this, the required irradiation over a one inch diameter test plane will probably require a transient (pulsed) system.

A pulsed system would reduce costs considerably by reducing or eliminating the requirement for water cooling, by requiring a less complex power supply and by eliminating the large shutter assembly in the source box. The transient-rated lamp could run in an idle state (10%) when not testing. It could then be driven at 70 Kw or more, stabilizing in 1 to 2 seconds. The sensor would be exposed to irradiation, and the lamp returned to the idle state.

On the following page is a table of the center line flux levels achievable with a 20, 25 and 32 Kw lamp along with their respective half-power radii to indicate relative uniformities.

LAMP (Kw)	OVERDRIVEN WATTAGE 3.5x	CENTER LINE FLUX (W/cm^2)	RADIUS AT HALF POWER (INCHES)
20	70	2133	.125"
20	70	1066	.20"
20	70	266	.40"
25	88	2353	.125"
25	88	1176	.20"
25	88	293	.40"
32	112	2559	.125"
32	112	1279	.20"
32	112	318	.40"

These figures are based on very conservative first estimates of efficiencies. A more complete design has been proposed by the supplier which would produce an irradiated one inch diameter area having the require 1140 W/cm^2 at the center line and 80% of center line intensity at a 0.5" radius, by simply defocusing the optics and spreading out the irradiated beam.

Calibration System Commissioning

After final assembly but before use in actual calibrations, the proposed system must be commissioned. During this process all sources of error in measuring heat flux and temperature will be identified, and the expected measurement precision and accuracy will be estimated. Final calibration procedures will be written, and final adjustments made to hardware and software. Most of the commissioning process will take place before installation in the sponsor's site, but some steps will be repeated after installation. The following is a brief description of the commissioning process.

1. A number of commercial heat flux sensors will be purchased and submitted to NIST for calibration. After NIST certification, these sensors will be used during system commissioning to measure and profile the radiative source. After commissioning they will be used as the system standard sensors.

2. Both sensor mounting stages will be instrumented with thermocouples and subjected to heating cycles in air and under

vacuum, measuring the time required to stabilize them at temperatures up to the specified maximum of 815°C. The accuracy of closed loop temperature control will be measured for each stage. The rate of decrease of temperature in air and under vacuum, starting at the maximum temperature, will be measured for each stage. These tests will be performed with the instrumented plug in place, but without a heat flux sensor mounted in it. The Compaq computer will be used for monitoring and control of these tests.

3. The positioning accuracy of the swing arm and drive assembly will be checked over the full calibration temperature range. Any thermally induced positioning error will be identified and compensated for in hardware or software. The ability of the swing arm to cover the full range of positions for profiling and calibration will be verified.

4. Operation of the shutters will be verified and opening and closing times measured.

5. A calibrated Heat Flux Microsensor or a cooled standard sensor will be mounted on one of the stages and used to profile the heat flux across the irradiation port with the source at various power levels. Data will be acquired for runs in both directions at various speeds. In the analysis of this data, the effects of sensor heating during the profiling process will be extracted. Actual levels of irradiated flux will be computed, to the limit of accuracy of the profiling sensors. The Compaq computer will control start and stop positions for profiling, stepping rates and data acquisition during these tests.

6. An error analysis will be performed on all data taken during commissioning, and the system accuracy will be tabulated.

Typical Procedure for Calibrations

An important part of any system specification is the description of how the system will be used in practice. Often the potential of a measurement system is not fully realized because procedures which must be followed in using it are intricate, time consuming or counter-intuitive. These problems can usually be forestalled by creating a clear and complete Description of Operation as a part of the initial specification. The following is an outline of what the Description of Operation for this system will include:

1. Set-up Procedures - Preparation of the system for a calibration cycle; cleaning, hardware and software testing, warm-up and preliminary measurements, if any;

2. Sensor Installation and Removal - How to mount and connect all types of sensors on the stage as standards or unknowns;

adjustment of the active region of the sensor in the correct position; pre-testing of sensor connections, closing the system, re-opening the system and removing calibrated sensors or standard sensors;

3. Computer Set-up - Procedures for entry of control information into the Compaq computer, file structure, data required for calibrations and data which will be generated.

4. Calibration Cycle Description - The complete sequence of events during an automatic calibration cycle as depicted in Figures 14 and 15.

5. Error Indications and Messages - Indexed list of all anticipated error conditions with instructions for correction or recovery; manual intervention procedures for all parts of the calibration cycle

6. Calibration Data Reduction - Data analysis options provided by the software and output reports available on the system monitor and printer.

Corrections for Re-radiation During Calibration

Heat flux from re-radiation of the sensors may reach levels as high as 8 W/cm^2 at 815°C. For tests at low heat flux, re-radiation could introduce significant errors in calibration. We have developed a method which can correct for re-radiated heat flux and eliminate these errors. The method is described below.

1. Irradiate the standard sensor, unheated, to determine q_{cold}.
2. Irradiate the unknown sensor, unheated, with q_{cold} and record the output, E_1.
3. Heat the unknown sensor to the temperature at which calibration is desired and record the output, E_2, from re-radiated flux q_{rerad}.
4. Irradiate the unknown sensor with q_{cold} at the same temperature and record the output, E_3. The sensor actually receives a flux of $q_{hot} = q_{cold} - q_{rerad}$.

A quadratic equation for the relationship above can be solved thus:

$$S_{hot} = \frac{E_3}{q_{hot}}$$

$$q_{hot} = q_{cold} - q_{rerad}$$

$$q_{rerad} = E_2 * S_{hot}$$

$$S_{hot} = \frac{E_3}{q_{cold} - E_2 * S_{hot}}$$

$$E_2 * S_{hot}^2 - q_{cold} * S_{hot} + E_3 = 0$$

Microwave-Driven Source

High intensity arc lamps are conventionally used as radiant sources for heat flux sensor calibration. These lamps have some drawbacks, however. They are physically large, consume a lot of power, and can be very costly. Even so, the properties of arc lamps are well known. For this reason we have selected this type of lamp for the proposed Phase II heat flux calibration system.

There is an alternative source which could provide an equivalent amount of radiant energy at lower cost. This type of source has never been used for heat flux sensor calibration. While capital and operating costs for the alternative could ultimately be less, it would take a substantial effort to achieve an equivalent working knowledge of this source.

The alternative source is a microwave-driven lamp manufactured by Fusion Imaging Systems. We saw an example of this type of lamp during our visit to NIST on September 3, 1992. The unit we saw was their HI-IQ type ultraviolet source, designed for UV curing of photoresists on silicon wafers. In Progress Report No. 1 we proposed that this lamp be considered as a calibration source. The envelope of this lamp is spherical. This is beneficial in the optical design of a calibration source because the lamp has no filament shadow. The maximum output of the HI-IQ lamp is 2000 watts. If the energy of a single lamp were concentrated on a 1" diameter area (5.07 cm^2) with 90% efficiency, the resultant heat flux would be 355 watts/cm^2. To achieve the objective of 1136 watts/cm^2, a cluster of (at least) 3 lamps would have to be used. However, before such a calibration source design could be tested, the supplier would have to resume manufacturing of the lamp, which has been discontinued.

Fusion Imaging Systems currently offers a microwave-driven lamp which has a linear bulb. The bulb is held in a two dimensional elliptical reflector and encased in a system housing as shown in Figure 11 of Progress Report #2. Bulbs rated at 600 watts/inch are available in ten inch lengths and are less than one inch in diameter. Because of microwave drive requirements, the reflective focusing apparatus surrounding the bulb is an essential feature of these lamps. The reflector focuses the light onto a narrow line whose length and width are equal to those of the bulb. This line is 2.1 inches from the exit of the reflector, as shown in Figure 12

of the same report. It might be difficult to design an optical system which would collect this beam and focus it on a 1" diameter area with an intensity of 1136 watts/cm².

The radiant energy of an array of (for example) four of these lamps might be easier to collect. Such an array would produce a 20 inch diameter area of radiation, which could be collected by a conical integrator. This type of integrator is known to be very lossy. Using four linear sources in an array would theoretically supply 21.6 Kw into the integrator. Only 25% efficiency would be needed to achieve the desired intensity. This may be possible, but it would require that the array of lamps operate as efficiently as a single lamp.

Microwave-driven lamps radiate in the range of .2 to 0.4 μm. To be used as a calibration source for heat flux sensors, we would have to convert the ultraviolet energy into heat. Black paint on the face of the sensor will absorb approximately 90 to 95% between 0.25 and 1 μm. This approach might have possibilities but would require extensive engineering, including special optics design. The unit cost of linear microwave-driven lamps from Fusion Imaging Systems is approximately $11,000. Appendix D is a copy of the specifications for these lamps. A high quality conical integrator of the required dimensions would cost more than $10,000.

We would have to have a high level of cooperation from Fusion Imaging Systems to investigate this source for use in heat flux sensor calibration. This vendor has not measured the infrared output of their lamps and has not tried to combine them in any type of array. We proposed some experiments at their facility which would result in useful information for them as well as us. However, to test an array of lamps, we would have to purchase them.

Task 2 - Heated Graphite Block Calibration System

A heated graphite flat plate or block is sometimes used as the radiation source for heat flux calibrations. There are many advantages to this type of source. A standard heat flux sensor can be placed on one side of the graphite block and the sensor to be calibrated on the other side. Providing that the two sensors have the same viewing angle and distance from the block, and the emissivity of the block is the same on both sides, the standard and the unknown will experience the same level of heat flux.

We explored possible use of this type of source for high temperature, high heat flux calibrations. To elevate its temperature, the sensor being calibrated could simply be irradiated by the source for a long time. At high heat fluxes the sensor would have to respond rapidly for calibration to be accurate under these transient conditions. Alternatively, a separately controlled source of heat could be applied to the sensor being calibrated, as described in Task 1.

We investigated high temperature calibration possibilities with flat plate and tube furnace configurations. Thermogage Incorporated sells such systems for calibration of heat flux sensors. A 48 Kw graphite tube furnace, their most powerful system, can reach 3320°C. This system is used to calibrate Gardon gages against an optical pyrometer. Since the radiation field of the tube is the same at both ends, the Gardon gage and the pyrometer are subjected to the same conditions. The calibrated Gardon gage is then used to calibrate other sensors using a heated graphite flat plate. Both calibration systems are limited in maximum temperature by the sublimation point of graphite. Graphite sublimes at 3600°C in an inert atmosphere. Thermogage uses their tube furnace system with an inert gas flowing through it, but the graphite still degrades rapidly at the high temperatures.

The calibration temperature and heat flux levels called for in this contract are both very high. The Stephan-Boltzman law predicts the source temperature for a heat flux of 1136 W/cm² (1000 Btu/ft²-sec) as 3762 K (3489°C), under ideal conditions. To achieve the same flux with a maximum sensor temperature of 815°C, the source must be at 3769 K (3496°C). These values fall just below the theoretical sublimation temperature of graphite. At these temperatures graphite will slowly degrade, even in a vacuum. This would greatly reduce the reliability and accuracy of the calibration system. The temperature restriction imposed by graphite sublimation would eliminate any possibility of further increasing the heat flux capacity of the system. While the graphite flat plate method may be viable for a lower range of heat fluxes, we do not recommend it for accurate calibrations at the limits called for in this contract. Even so, the flat plate may be used as a method to transfer standards or as a comparison method for another system since it has been accepted for some time.

Task 3 - Convection Calibration System

Convection calibration methods are difficult to employ because one cannot accurately predict the heat transfer coefficient for many flow situations. The best known method (by Diller) is to use a jet impinging on a semi-infinite flat plate to produce a predictable and repeatable flow field. We investigated the potential of this method for producing heat fluxes on the order of 56.8 W/cm². One proposal was to use a Mach 2 free jet supplied by a blow-down wind tunnel. We found that the development of a system like this, including controls for the temperatures of the sensors being calibrated up to 815°C, would be very slow, difficult and expensive. Since the contract objective is to develop a system which will be useful in the short term, we applied little direct effort to this approach. Instead, we assisted Virginia Tech in the development of more accurate low heat flux convection calibrations.

Virginia Tech developed a convection calibration apparatus for Heat Flux Microsensors which used a larger free jet than the previous

system.[5] The jet diameter was increased to 1.5" to achieve a uniform heat flux across the 1 inch diameter substrate containing the sensor. The free jet was formed by an orifice in a steel plate mounted at the exit of a blower assembly, as shown in Figure 16. An insulated box with a flat front surface was mounted in the path of the jet, 3 orifice diameters downstream from the steel plate. The sensor to be calibrated was mounted in an aluminum tube insulated by wood. A silicone rubber heater, powered by an SCR temperature controller, was wrapped around the tube. The temperature of the sensor was monitored using the RTS on the substrate surface. Calibrations were performed by controlling the temperature of the sensor at a variety of set-points while the jet impinged on the surface.

Virginia Tech found the heat transfer coefficient for this flow configuration to be 205 ± 2.3 W/m²-K, using a calibrated Gardon gage. Multiplying this value by the difference between the temperatures of the free jet and the Heat Flux Microsensor surface, VPI determined that the standard deviation in measuring sensitivity of the microsensor was 6%. The maximum heat flux attained with the free jet was approximately 0.68 W/cm². Virginia Tech also calibrated a Schmidt-Boelter gage with this apparatus. and the measured sensitivity was within 4% of the manufacturer's value. In all tests the sensitivity was corrected (2%) for radiation from the sensor.

Virginia Tech assembled another convection calibration apparatus by placing the same insulated box, with the sensors on its upstream face, in the test section of a low speed wind tunnel. The box was located in a region where the boundary layer of the tunnel was fully developed. Heat flux was set at different steady state levels by adjusting the temperature of the sensor surface. The maximum temperature difference attained was 40°C. Using the calibrated Gardon gage, the heat transfer coefficient was determined to be 52.8 ± 2.5 W/m-K. The Heat Flux Microsensor was calibrated to within a standard deviation of 10%. The standard deviation of the Schmitt-Boelter calibration was 7% and the average of all readings was within 2% of the manufacturer's value. The maximum heat flux attained with this apparatus was 0.2 W/cm². The values of gage sensitivity were generally within 6% of those determined using the free jet configuration.

These are examples of convective heat flux sensor calibration methods. While the maximum heat fluxes they can attain are quite low, these methods can be used to compare a sensor's performance in different heat transfer modes. The information acquired by these methods can be useful in the research described in Task 4.

Task 4 - Separation of Radiative and Convective Heat Flux

In one existing method for separation of radiative and convective heat flux, measurements are made with a heat flux sensor placed behind a transparent window which shields the sensor from convection. These measurements are compared to measurements made without the window, and the difference is an indication of the convective heat flux. This method is difficult to employ in some environments, such as in combustion testing. We now propose a much simpler method, which will allow the heat flux sensor to be exposed directly to the test environment. Only a single test will be required to measure both convective and radiative heat fluxes as a function of emissivity.

Figure 17 shows a Heat Flux Microsensor adapted for separation of radiative and convective heat fluxes. It contains three sensors; two of which measure heat flux and one which measures temperature. The two heat flux sensors are coated with different emissivity control layers, one of relatively high emissivity and the other of low emissivity. For example, one sensor may be coated with a black, light absorbing paint ($\alpha \geq .7$) and the other by a mirror coating ($\alpha \leq .3$). The emissivity of each coating will be measured as a step in the calibration of this microsensor.

To separate the radiative and convective components of heat flux as a function of emissivity, this microsensor could be used in the conventional manner. It could be designed as a probe or applied directly to the surface. During an experiment, signals of the two heat flux sensors and the temperature sensor would be separately recorded. Processing of the signals for separation could be done in real time or during playback of the raw data. The graph in Figure 18 shows how the separation is achieved. The amplitude of each signal is plotted as a point on the respective vertical line for the emissivity of its sensor. A straight line is then drawn through the points for the two different emissivities, describing signal strength as a function of emissivity. The intercept of this line and the vertical line for zero emissivity is a computed value for convective flux, since at zero emissivity the radiative component is zero. The intercept of this line and the vertical line for an emissivity of 1.0 is a computed value for total available flux. The difference between the computed total available flux and the computed convective flux is the radiative flux. The straight line shows the relationship between total flux and emissivity of a surface in that environment. If temperature corrections are required for behavior of the emissivity control layers or changes in the sensitivity of either heat flux sensor, the signal of the RTS can be used for this purpose. Further corrections may be required for the variation of emissivity with wavelength of the emissivity control layers.

There are many ways to test the accuracy of this separation method. For example, the test rig shown in Figure 19 combines a pure

radiation source and a pure convection source, each independently controlled and calibrated. The total heat flux signal will be the sum of the two independent heat fluxes. With this rig, a sensor can be calibrated with any combination of temperature, convective flux and radiative flux.

Task 5 - Investigation of Heat Flux Standards

At the beginning of the Phase I contract Vatell representatives visited the National Institute of Science and Technology (NIST). During this visit we described the work proposed for our contract and discussed the design options for a calibration system. Progress Report #1 contains the notes of this meeting. One of the topics we discussed during the visit was heat flux standards. According to NIST there is no heat flux standard. While calibrations performed there have high accuracy, this is not achieved by comparison to a standard. The radiation source used for calibration is itself calibrated using a radiometer, which is an optical radiation standard. The reason why NIST heat flux calibrations are limited to 4 watts/cm^2 is that the radiometer is limited to this level of radiant flux.

The only true thermal standard is the temperature at the melting point of gold. NIST agrees that a heat flux standard is needed but it would only be of value if it could be directly related to measurements of temperature or electrical power. The present accepted "standard" for high heat flux is the slug calorimeter. This device uses the time history of the temperature gradient through a slug of a known, pure material for a calculation of heat flux. Its measurements are as closely related as any to the standard for temperature, and this is why it was chosen as the reference standard for the proposed calibration system.

Vatell had initially proposed an improvement to this design which would use thin film temperature sensors distributed over the surface of the slug material. Upon further investigation we believe that we can develop a potentially more accurate method. This method relies on the unique capability of a single Heat Flux Microsensor to measure radiated and conducted heat flux. With this capability its heat flux signal can be related to a precise measurement of electric power.

The proposed heat flux standardization method is derived from the Controlled Heat Flux Source (CHFS) which was developed for a thermal conductivity and diffusivity measuring application. Figure 20 is a diagram of this device. Referring to the diagram, a thick film resistance heater is printed on the top surface of a thin (.020") aluminum nitride substrate. The pattern is designed to produce uniform heating of the substrate. Power to the heater is controlled and measured by a DC power source. Heat generated in the resistance heater is dissipated in the steady state by convection and radiation from the top of the substrate, and by

conduction through the substrate. A Heat Flux Microsensor is sputtered onto the surface of the substrate opposite the heater.

To use this device for calibration it will be thermally coupled to the end of a copper (or other highly conductive) rod (Figure 21) so that the electrically produced heat is conducted out of the substrate and into the copper. The Heat Flux Microsensor to be calibrated is sputtered on the face of the copper rod in the conventional manner. The surface area of the copper rod must be precisely known so that the heat flux can be calculated from the total power. Heat flows across the contact resistance between the substrate and copper rod and through the Heat Flux Microsensor on its face. The heat is removed from the calibration apparatus by cooling water which circulates through passages in the copper rod.

An equivalent thermal circuit representing the calibration apparatus is shown in Figure 22. We performed a thermal analysis to estimate the parasitic convective and radiative losses and compare them to the heat conducted through the face of the copper rod. With good insulation these losses are negligible, and can be estimated with good accuracy.

The sensor on the aluminum nitride substrate makes it possible to measure the actual contact resistance between the substrate and the copper rod. If the contact resistance is above a certain level, the radiative and convective losses may become appreciable in the determination of heat flux. If the contact resistance is below this level, most (99%) of the heat produced by the heater will flow into the copper rod. The sensitivity of the Heat Flux Microsensor on the copper rod can be calculated from its voltage signal, the heater power minus parasitic losses, and the area of the copper rod.

After calibration in this manner, the Heat Flux Microsensor on the face of the copper rod can be used to calibrate a radiation source. The radiation source can then be used for calibration of other sensors. The CHFS can also be used to directly calibrate Heat Flux Microsensors which have been applied to other surfaces, providing they are sufficiently flat to achieve uniform contact resistance. A portable version of the CHFS could be designed for field calibration of heat flux sensors which are installed in an experimental apparatus or in other applications.

The following calculations illustrate that the losses from radiation and convection are negligible in a typical case with contact resistance maintained below .000141 °K/W. The maximum temperature of the heater is assumed to be 400°C and $T_{atm}=T_{wtr}=25°C$.

Conduction

$$q_{cond}=\frac{T_{htr}-T_{wtr}}{[(\frac{L}{kA})_{AlN}+(\frac{L}{kA})_{CR}+(\frac{L}{kA})_{cu}+(\frac{1}{hA})_{wtr}]}$$

$$(\frac{L}{kA})_{AlN}=.00562°K/W$$

$$(\frac{L}{kA})_{CR}=.000141°K/W$$

$$(\frac{L}{kA})_{cu}=.0246°K/W$$

$$(\frac{1}{hA})_{wtr}=.116°K/W$$

The total thermal resistance through the conductive path is,

$$R_{total}=.00562+.000141+.0246+.116$$

$$R_{total}=.146°K/W$$

The conductive heat flux is,

$$q_{cond}=2566W/m^2$$

Convection

The convective flux will be considerably less than the conductive flux. The convective thermal resistance and losses calculated below are for atmospheric conditions.

$$h_{atm}=\frac{Nu*k}{L}$$

$$Nu_{atm}=.372Ra^{.27}$$

$$Ra_{atm}=Gr*Pr$$

$$Ra_{atm}=966.6$$

$$Nu_{atm}=2.38$$

$$h_{atm}=15.25 W/m^{2\circ}K$$

$$R_{atm}=101.6^{\circ}K/W$$

The heat lost to convection in atmosphere is,

$$q_{conv_{atm}}=3.7W$$

Radiation

An estimate of the losses by radiation is:

$$q=\sigma\epsilon A(T_s^4-T_{atm}^4)$$

Assuming a worst case, $\epsilon=1$,

$$q=(5.67e^{-8}W/m^{2\circ}K)\,(1)\,(6.45e^{-4}m^2)\,(673^4-300^{4\circ}K)$$

$$q=7.21W$$

A summary of the results is listed below.

Mode of Heat Transfer	Heat Transferred (watts)
Conduction	2566
Radiation (loss)	7.21
Convection (loss)	3.7

It is evident from the relative magnitudes of heat transferred that extreme measures for insulation (e.g. vacuum) are not necessary in this standardization technique to minimize convective losses. The sum of all the losses (radiative and convective) make up less than 1% of the total power. However, a vacuum may be employed to make convective losses more negligible, and a radiation shield could be inserted to further reduce radiative losses.

In one respect this method is similar to calibration by radiation. The uniformity of heat flow through the surface containing the Heat Flux Microsensor is a primary factor in its accuracy. Thus the uniformity of thermal contact between the aluminum nitride and copper and the uniformity of heat produced by the heater will both affect the accuracy which can be achieved in practice. These will be the dominant sources of error because it is possible to measure

electrical power and surface area to at least four significant figures. With good control of heating and contact resistance uniformity, this method may provide a calibrated heat flux standard with an accuracy of ±1% or better.

An experimental investigation of conductive heat transfer at the interface between two flat surfaces showed that a reduced diameter portion of an aluminum nitride substrate produced increased heat fluxes with adequate uniformity, as indicated in Progress Report #3. The reduced diameter portion of the substrate served to concentrate the flow of heat and increase the heat flux to levels approaching those of radiation calibration sources. Three concentration geometries were analyzed by finite element modelling to determine the best geometry for adequate uniformity. The geometries are shown in Figures 23-25 with their corresponding steady state heat flux gradients.

Task 6 - Investigation of Sensor Radiation Response

In this task we were concerned with two aspects of Heat Flux Microsensor calibration using radiation sources. The first is the disruption of heat flow and the change in surface temperature distribution caused by the sensor. Since the sensor covers only a part of the surface area which is illuminated during calibration, it is important to know how much of disruption and change there is. The area that is prescribed to have uniform incident flux is 1 inch in diameter. Sensors that are smaller than this area and are of materials different from the surrounding surface will cause a noticeable temperature discontinuity. The substrate of the Heat Flux Microsensor is uniform in properties and equal in area to the area of uniform irradiance. Because the sensor elements are made by thin film processes, they have negligible heat capacity and do not cause a measurable temperature disruption.

The second aspect of radiation response is the effect of wavelength. An uncoated Heat Flux Microsensor responds differently to radiation at different wavelengths. Most of the sensors that are to be calibrated will be coated with a black absorbing coating. A thin film sensor has the advantage that a wide variety of coatings can be applied.

Task 7 - Definition of Calibration Controls

The proposed calibration system will be fully controlled by a Compaq desktop personal computer. This computer will provide a platform to control the calibration process while collecting and analyzing data. Software will coordinate all systems within the computer. Three main functional groups can be defined: 1) data acquisition, 2) motion control, and 3) temperature control. Each of these functional groups will have its own special interface to the Compaq computer.

Data Acquisition

The data acquisition portion of the system will consist of a custom designed EISA plug-in printed circuit card. This card will be based on the current Vatell data acquisition card. The card will plug into a slot on the EISA bus of the computer, which will serve as its host and as the system's main control unit. Figure 26 is a block diagram of the card.

The card is partitioned into 10 main units: analog signal conditioning, an 8 channel analog multiplexer, a 14-Bit A/D converter, a 16-Bit input port, input signal conditioning, a 16-Bit output port, output signal conditioning, a 16-Bit counter, a crystal clock oscillator circuit, and interface/decoding logic. Each unit will be described briefly below:

1. **Analog Signal Conditioning**: This consists of the physical interface (connector) to the heat flux sensors in the calibration chamber and analog signal conditioning electronics (i.e. amplifiers, filters, etc.) which will vary with the type of sensor.

2. **8 Channel Analog Multiplexer**: An Analog Devices AG508A 8 Channel Analog Multiplexer will be used. This will select the sensor signal for sampling by the A/D converter.

3. **14-Bit A/D Converter**: An Analog Devices AD7871 A/D converter will be used for this function. It is a complete monolithic successive-approximation A/D circuit with a maximum sampling rate of 100KHz and a built-in sample and hold circuit. Its input range is -3 to +3 volts.

4. **16-Bit Input Port**: A Texas Instruments (TI) 74AC16374 16-Bit D-type edge-triggered flip-flop chip will be used as a digital input port. This is one of TI's new surface mount 16-bit chips which saves considerable board space over any other equivalent circuit. This port will be used to monitor system conditions (stage position, shutter position, alarm warnings, etc.).

5. **Digital Input Signal Conditioning**: This will consist of the required physical interface and any necessary isolation or interface circuits (opto-isolators, 12V or 4-20mA loop to TTL level conversion, etc.) to convert sensor data into digital signals.

6. **16-Bit Output Port**: This port actually consists of two 8-bit ports. One is a Texas Instruments 74F374 8-bit D-type edge-triggered flip-flop chip and the other is a National Semiconductor DP8311 Peripheral driver chip. This combination allows control of standard TTL loads (the 74F374) and with the DP8311 control of heavier loads associated with relays and

other devices. This port will be used to trigger external events such as shutter openings, motion control, etc.

7. **Digital Output Signal Conditioning**: This will consist of the required physical interface and any necessary isolation or interface circuits to transmit digital signals to their appropriate control devices.

8. **16-Bit Counter**: Two Texas Instruments 74LS590 8-bit counter chips will be used to implement a 16-bit counter. This counter is used for accurate timing of the data collection process.

9. **Crystal Clock Oscillator Circuit**: This will consist of a quartz crystal controlled clock at preset frequency (typically 20-50KHz), 4 J-K flip-flops (Texas Instruments 74F109s) used as a divider, and a Texas Instruments 74F153 digital multiplexer to select the frequency delivered to the counter.

10. **Interface/Decoding Logic**: The interface logic will be a Texas Instruments 74ACT16245 16-bit bus transceiver chip. It is a new surface mount chip from TI and saves considerable board space compared to older solutions. The decode logic is in 2 Texas Instruments PALs (TIBPAL20R6s). By using programmable logic for the decode, minor changes can be made in the system configuration, and debugging is easier.

Motion Control

The motion control section will consist of 3 parts: 1) motor indexer and drive, 2) motor and feed-through, and 3) shutter system. To exchange sensors within the vacuum chamber in the field of radiation, the sensors are mounted on a movable stage. The motor, its feed-through (into the vacuum chamber), the indexer and its drive unit will all work together to provide such movement. The shutter system will be used for timing the exposure of sensors to the radiation source.

A Galil DMC-1000 will function as the motor indexer. This is a plug-in card that interfaces to the Compaq personal computer through the computer's EISA bus. This card is a specialized 32-bit microprocessor based motion control system. It can be programmed by the host computer once and will execute this program independently of the host. The card has several external digital input and output ports for external triggering. This combination of external triggering and independent program execution will facilitate precise motion control (either sensor profiling or centering of the sensor under the source) without requiring excessive host computer overhead.

The indexer and drive have two main purposes: 1) placement of

sensors by rotation of the swing arm and 2) precise continuous motion of a sensor across the exposure port for source profiling. The selected motor and drive, used with this indexer, will allow profiling with a resolution of better than .021 inches. This indexer will be combined with a Compumotor PK130M Ministepping Drive.

The Compumotor PK130M drive will be matched to a Compumotor PK130-106-178 ministepping motor. This motor will produce up to 960 oz-in of torque and is capable of speeds up to 3000 RPM. Combined with the PK130M drive and the Galil DMC-1000 motion controller, it is capable of 2000 steps/rev. at 3000 RPM. With a 6.59 inch lever arm connecting the sensor stage to the motor, the each step of the motor is equivalent to 0.0207 inches of travel across the source. This motion will be coupled into the vacuum chamber by an MDC 652100 CF flange high speed rotary feed-through.

The shutter system consists of two shutters and their controlling mechanisms. Figure 27 diagrams the shutter opening process. First, the large shutter opens, exposing the smaller shutter to the radiation source. As soon as full opening of the large shutter is detected by a limit switch, a Lucas Ledex 810-641-323 rotary solenoid will be operated, opening the smaller shutter. This shutter will open within 50 milliseconds, exposing the sensor within the vacuum chamber to the radiation source. Computer controlled timing will ensure that the small shutter is open no longer than needed. Immediately after the small shutter has been closed, the large shutter will be closed, also.

Temperature Control

Prior to exposure to the radiation source, the stage holding the sensor within the vacuum chamber will be heated to a predetermined temperature. Stage temperatures will be controlled by a single 2 channel PID controller in combination with 2 SCR power controllers.

Several commercially available controllers meet the requirements of this system - either Honeywell's UDC 5000 or Eurotherm's Model 906D. Properly equipped (auto-tune capability, 2 independent channels, computer interface, 4-20 Ma output and alarm circuitry). Both units are RS-232 compatible, which means that they can be fully controlled by the Compaq Computer.

Each PID controller will control an SCR heater power controller. Payne Engineering makes several suitable SCR units. Their Model 18D-1-20I-11C would be the most likely choice. It is a single phase, 60Hz, 115 Volt, 20 Amp, phase angle switched SCR controller which accepts 4-20 Ma current control signals from the PID controller. A zero switched SCR, would produce less power line noise and harmonics. Two of these units will be needed to control the heaters on the sensor stages in the vacuum chamber.

In coordinating system operation the Compaq computer will pass set-point information to the PID controllers. These will drive the SCR heater controls, which will bring the substrates accurately and precisely to the desired temperatures. Once stable, the heaters will be turned completely off and the computer will go into the calibration test mode. Once calibration data for that particular temperature and heat flux level have been taken, the PID controllers will be given the next set-point. The process will repeat itself until completion of the last test.

Software

Using object oriented programming and Borland's Turbo Vision framework, a professional windowed user interface will be developed. This interface will allow the user full control of the data-acquisition process without getting bogged down in details of process or hardware. All processes will be controlled by the computer and the user will be prompted for any information which is needed before testing. The emphasis in software design will be on user interface convenience, total system automation, and meaningful data display.

Appendix A - Proposed Equipment List and Costs

Quantity	Description	Supplier	Cost
1	Pulsed light source	Spectro	$324,000
1	custom chamber w/tabs DWG#B93003	Nor-Cal	$1200
1	custom flange CF12 w/viewport DWG#B93004	Nor-Cal	$600
1	custom flange ISO-250-000-OF DWG#B93005	Nor-Cal	$600
1	rotary motion feed-through (F.T.) CF1.33 mini	MDC	$350
2	dual fluid baseplate F.T. mount in 1.00"D through-hole	ISI	$100 ea.
1	4-pin medium current electrical CF2.75	Nor-Cal	$290
2	8-pin instrumentation F.T. CF1.33 mini	Nor-Cal	$135 ea.
2	quartz viewport w/ 1.4"D view CF2.75	ISI	$200 ea.
1	quartz viewport for vacuum side CF2.75 seal on opposite side	ISI	$300
1	DUO 1.5A rotary pump pumping time atm to 1 torr(3 min.)	Balzers	$800
1	linear rail system blocks/rails/supports	Thompson	$248
2	reflective radiation shields gold plated quartz 4"D x 4"L	EMF	$200 ea.
2	custom machined boron nitride	Carbor.	$150 ea.
2	custom machined nickel plugs	Local	$50 ea.
4	flexible stainless steel tubing 0.25"D x 2.0"L	MDC	$35/inch
1	indexing controller	Galil	$1295
2	Stepping motor	Compu	$3012
2	Solenoid	Ledex	$150 ea.
1	Computer	Compaq	$3851
1	Plug-in Card	Vatell	$3000
Total			$341,796

Note: The above are costs for material only, based on preliminary design estimates. Design and other preparation costs are not included. The Phase II proposal will include these.

Appendix B - Phase II Design, Fabrication and Delivery

The proposed calibration system design which is described under Tasks 1 and 7 in this report is preliminary. Only a complete design process will identify the design variables and system features which are important to achievement of the contract objectives. In a Phase II continuation of this project, we will carry out such a design process, including the following steps:

1. Initial design review - The preliminary system design will be presented, reviewed and analyzed to insure that it is consistent with the contract objectives. The required changes will be made to specifications and plans.

2. Project planning - A schedule for all design, fabrication and test activities will be written, and project controls set up for monitoring of progress.

3. Data Gathering - Full details of all equipment needed, all requirements for coordination with other systems, and the current status of standards and methods for heat flux calibration will be assembled.

4. System Design - A mechanical assembly drawing, a block diagram of the electronics and a software flow chart will be made.

5. The mechanical assembly will be subjected to kinematic and thermal analysis, the latter by finite element methods.

6. Requirements for computing capacity, data flow, timing and memory will be determined from the block diagram.

7. The software flow charts will be analyzed to identify potential operating problems.

8. In preparation for beginning the detailed design, a final design review will be held with the sponsor.

9. The system will be constructed and commissioned. Manuals, parts lists and spares recommendations will be written and assembled.

10. The system will be delivered, assembled at the sponsor's site, and subjected to final tests.

Appendix C

Spectrolab

SPECTROSUN® MODEL X-200 SOLAR SIMULATION SYSTEM

A system of artificial sunlight for large area illumination.

Pg 7 of 11

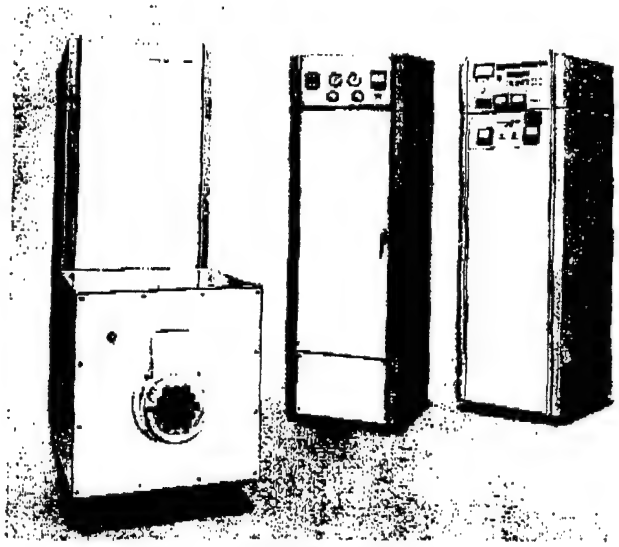

Five basic components make up the Model X-200 system: a xenon source module, an optical system, a power supply, a module controller and compact coolant conditioning unit.

An artificial sunlight source designed to illuminate large areas, the Spectrosun® Model X-200 Solar Simulation System projects at a distance of 140 inches a hexagonal beam 50 inches across the flats . . . a beam that closely matches air mass zero sunlight at variable intensities up to two solar constants.

Its characteristics of beam uniformity, close spectral match and unattended operation for up to 400 continuous hours with precise electronic control of the beam output make the X-200 ideal for all types of sunlight exposure tests. The system is well suited to materials degradation work, solar power systems tests, thermal balance studies, photo-chemical reaction studies and similar projects.

The X-200 includes a source module and optical system housed in an environmental enclosure, a water-cooled power supply, a module controller and compact coolant conditioning unit. Operation is simple, with electrical interlocking to prevent danger to personnel or damage to the equipment.

A full range of available options adapts the X-200 system to almost any laboratory solar application.

THE SPECTROLAB X-200 SOLAR SYSTEM: The X-200 Spectrosun® is a versatile laboratory solar radiation source comprised of standard hardware designed and constructed to project a stable, highly uniform light beam that simulates the intensity and spectral content of solar energy at a specified target area. The X-200 is of a modular design to provide overall flexibility in the system arrangement necessary for individual facility requirements.

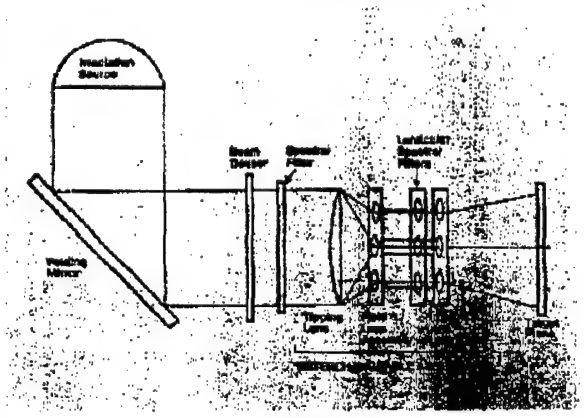

Optical schematic diagram, X-200 Solar Simulation System.

XENON SOURCE MODULE AND OPTICAL COMPONENTS ENCLOSURE: This module contains a xenon light source for illumination of the transfer optics in the X-200. It is designed around a compact, xenon short-arc light source which is adjustable over an input power range of 5 to 30 KW, mounted in a stress-free holder and fitted with micrometer adjustment controls in X, Y and Z axes.

In addition to its xenon light source and lamp holder, this module contains an automatic lamp starter, a high-efficiency, 22-inch electroformed nickel collector and all necessary thermal, electrical and environmental control systems for long-term, safe operation of the lamp.

OPTICAL SYSTEM: The optical components form a versatile package composed of a number of standard, interchangeable parts which can be combined and assembled to meet specific user requirements. The optical elements include the beam folding mirror, spectral filtering and the transfer optical package which contains the field and projection lenticular assemblies.

LC-52 POWER SUPPLY: This water-cooled, Spectrolab-developed module is a regulated, direct current power supply used to power the XM-300 Xenon Source Module with xenon compact-arc lamps operating with a high degree of regulation over input power ranges of 10 to 50 KW. The unit is designed to operate with its companion module, the MC-300 Module Controller, located atop the LC-52 Power Supply.

The compact LC-52 Power Supply has closed-loop control and low current ripple, closely regulated by monitoring the light output intensity and thereby automatically controlling the DC power output.

All solid-state circuitry associated with controls and monitors is contained in a submodular cabinet that can be removed from the power supply main cabinet for ease of maintenance.

Pg 8 of 11

XM-300 Xenon Source Module.

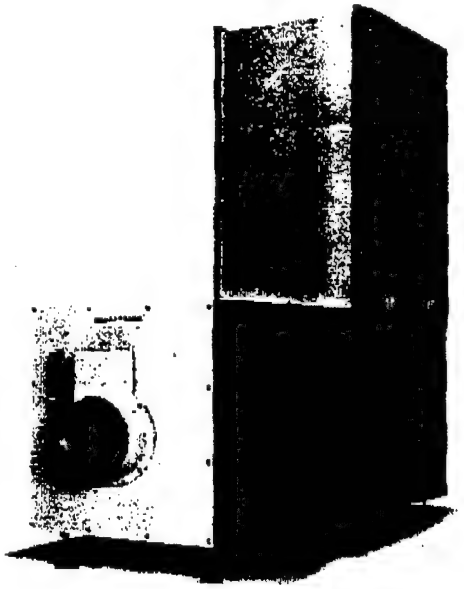

Xenon source and optics enclosure.

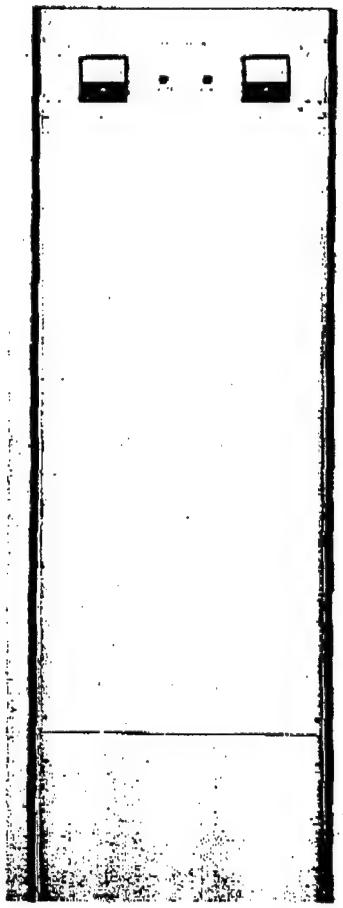

LC-52 Power Supply Module.

MC-300 MODULE CONTROLLER: A unitized control panel and cabinet assembly which provides a central operating facility, the MC-300 Module Controller performs these functions for the total system: manual control, automatic control, performance monitoring and malfunction and warning display. It employs all necessary control and interlock circuitry associated with operating an XM-300 source module and an LC-52 Power Supply.

All system operating controls are included in the individual units of the system. Each automatic control channel acts as a system interlock and interfaces with circuits which monitor critical system operation parameters such as electrical power levels, coolant flow and pressure, enclosure integrity, temperature and irradiance intensity.

COOLANT CONDITIONING UNIT (CCU): The CCU, Model CCU-HP5, is a compact system designed to provide environmentally controlled coolant to the XM-300 source module. It is a self-contained unit which provides the process fluid used as the heat exchange media for the lamp electrodes and energy absorbers within the source module. The CCU delivers process fluid at discharge flow rates at 300 psi outlet pressure with gravity feed to pump inlet of 5 gpm. It automatically de-ionizes and filters the heat exchange media as it is recirculated through the system.

In addition to its demineralization system, the CCU contains a dual disposable filter set, three-way temperature control valve and sensor system, a reservoir and pressurization system. It monitors pressures, flow rates, fluid conductance and temperature on a fully automatic basis and provides automatic alarm and interlock signals to protect the various components.

Pg 9 of 11

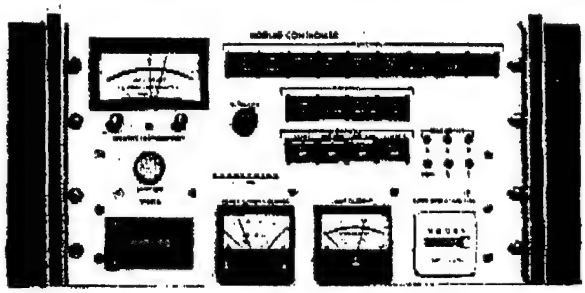

XM-300 Module Controller.

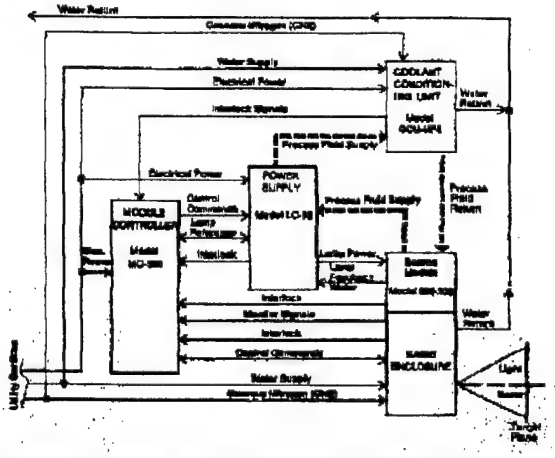

Functional block diagram of complete X-200 Solar Simulation System.

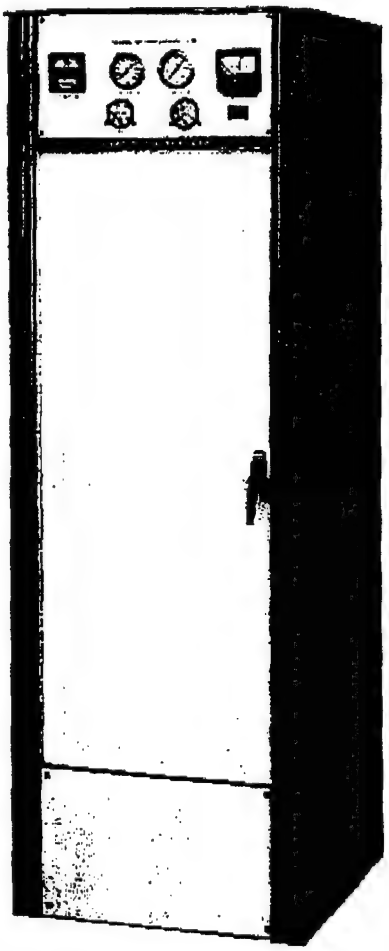

Coolant Conditioning Unit (CCU).

SPECTROLAB:
SPECTROSUN® MODEL X-200 SOLAR SIMULATION SYSTEM

SPECIFICATIONS AND PERFORMANCE DATA

X-200 Basic Enclosure

Light source:
Xenon short-arc lamp adjustable over nominal input power range of 5-30 KW.

Beam intensity:
Nominal capability: 1 solar constant irradiation (unfiltered) at target area of 20 sq. ft.

Beam orientation:
Horizontal. Vertical or inclined in special applications.

Beam uniformity
Spatial:
±3% with 2 sq. cm monitor.
Temporal:
Not to exceed ±2% for time periods of 100 milliseconds to 60 minutes.

Optics:
Quartz lenses; metal mirror; an overcoated aluminized Aconic Source Collector* with water cooling.

Spectral match:
0.25-2.7 micron xenon spectrum, as modified by optical elements of the system.

Accessory Features
Spectral filter:
Provides close match of simulator spectrum to the N.R.L. air-mass-zero solar spectrum.
On-axis collimating mirror assembly:
On-axis assembly complete with aconic collector assembly and primary mirror 23" diameter; assembly includes all mounting fixtures required.

Interchangeable lenticular lens sets:
Provides capability to produce a variety of beam characteristics to user specification.

Dimensions
Width:
29".
Depth:
82" (overall, including snout)
Height:
72".
Weight:
2,000 lbs.

LC-62 Power Supply

Output current:
150 to 650 amperes, adjustable to within ±5 amperes.

Output voltage:
30 to 80 VDC, adjustable to within ±2.0 VDC.

Output current ripple:
Less than 2% RMS (within the specified voltage and current operating range when operated with a 0.04-ohm external load).

Line regulation:
Output voltage variation does not exceed ±1% over time periods from 100 milliseconds to 1 hour with input line voltage variations of ±10%.

Dimensions (includes MC-300 Module Controller)
Width:
24".
Depth:
27".
Height:
72".
Weight:
1,200 lbs.

Coolant Conditioning Unit

Heat rejection:
30 KW (plus 50% excess capacity)

Fluid Temperature
Outlet:
115°F. (max.).
Inlet:
95°F. (max.).

Pressure
ΔP:
30 psi (max.).
Outlet:
300 psi (nominal).
Pressure drop (across heat exchanger):
20 psi (max.).

Flow:
5 gpm (plus 20% excess capacity).

Demineralization
Process fluid conductivity:
50 micromhos (max.).
Operational life cycle:
2,000 hours (min.).

Filtration:
Filter type:
Dual disposable element.
Particle size:
5 microns (max.).

Dimensions:
Width:
24".
Depth:
27".
Height:
72".
Weight (dry):
1,800 lbs.

*Pat. 3,445,551

Contact Spectrolab for further information on the X-200 System and how it can be adapted to your solar simulation needs.

SPECTROLAB A DIVISION OF textron INC. 12484 GLADSTONE AVENUE, SYLMAR, CALIFORNIA 91342 / TEL: (213) 365-4611

Pg 11 of 11

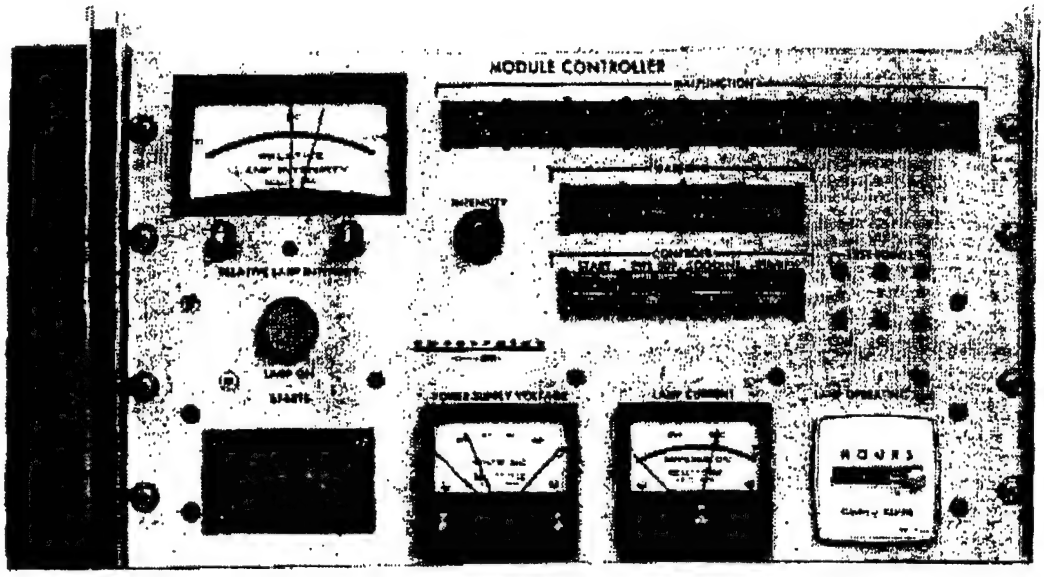

XM-300 Module Controller.

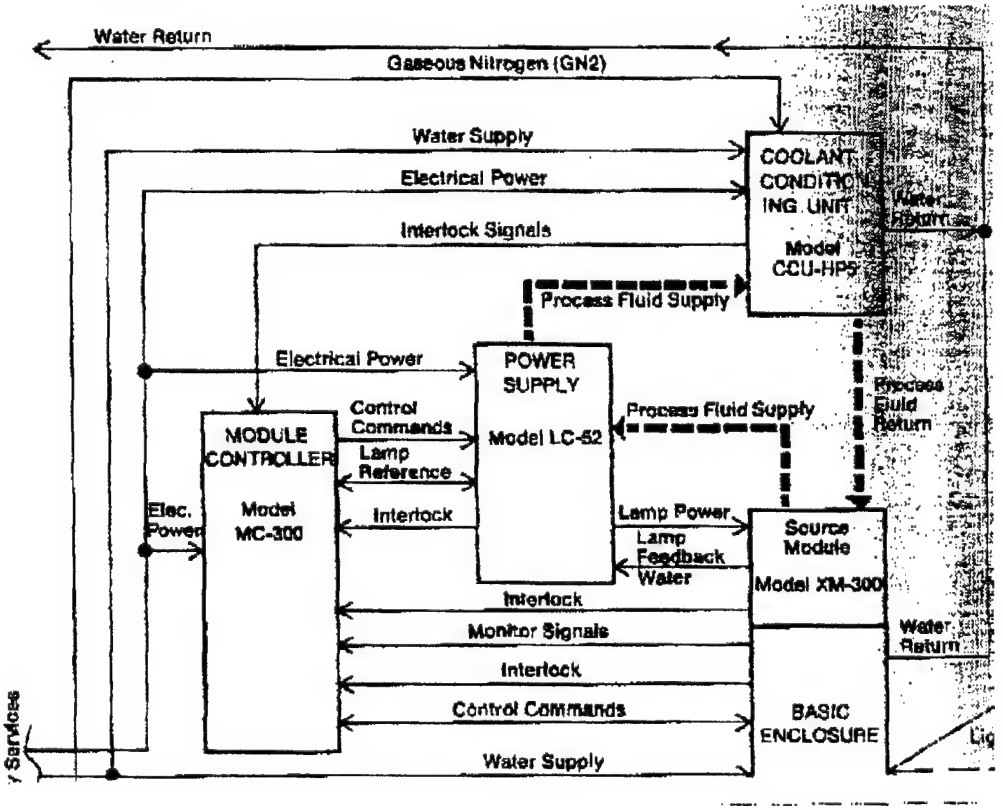

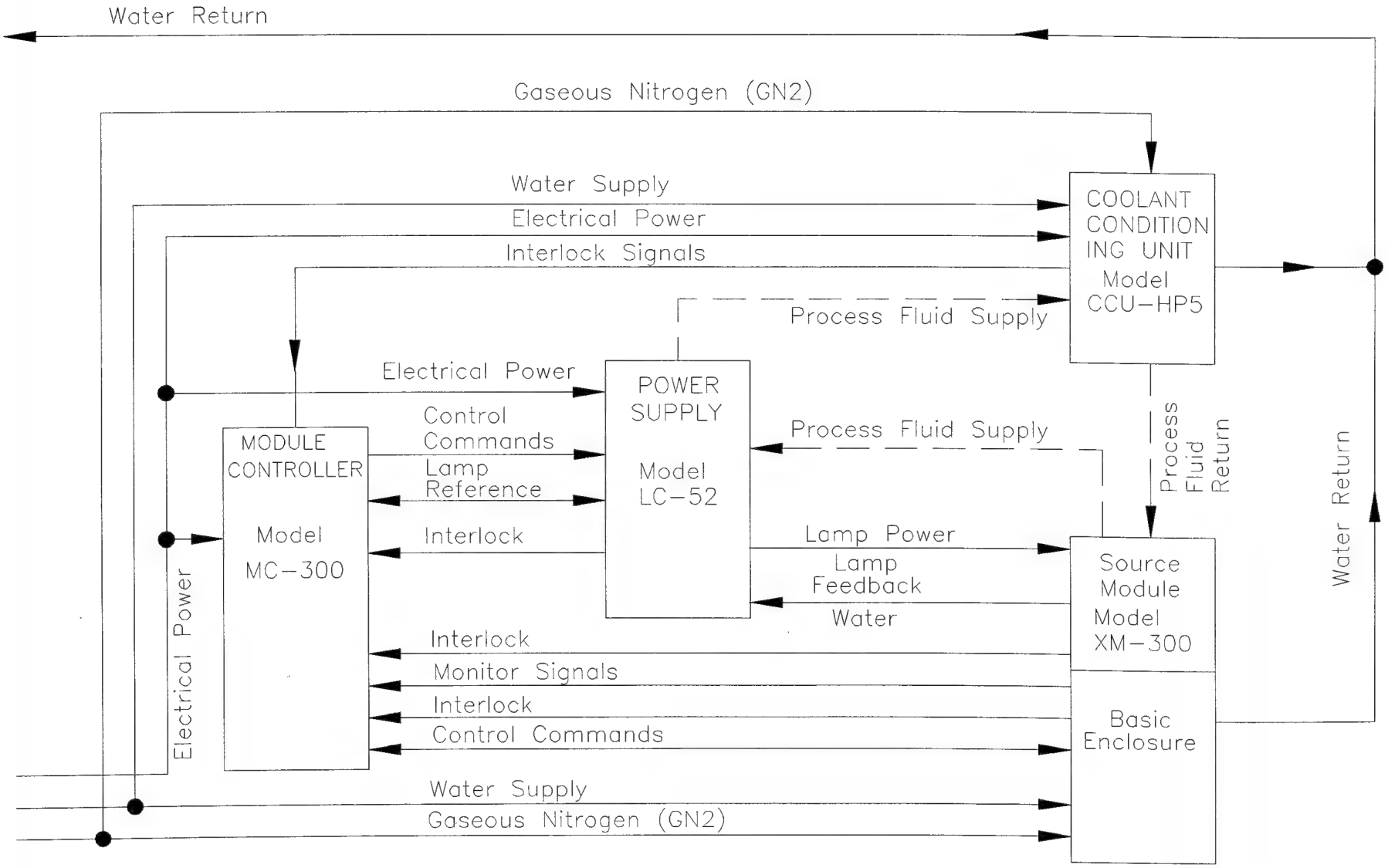
Water Return
Gaseous Nitrogen (GN2)
Water Supply
Electrical Power
Interlock Signals
COOLANT CONDITIONING UNIT
Model CCU-HP5
Process Fluid Supply
Electrical Power
POWER SUPPLY
Model LC-52
Control Commands
Lamp Reference
Interlock
Process Fluid Supply
Process Fluid Return
Water Return
MODULE CONTROLLER
Model MC-300
Lamp Power
Lamp Feedback
Water
Source Module
Model XM-300
Interlock
Monitor Signals
Interlock
Control Commands
Basic Enclosure
Electrical Power
Water Supply
Gaseous Nitrogen (GN2)

Appendix D

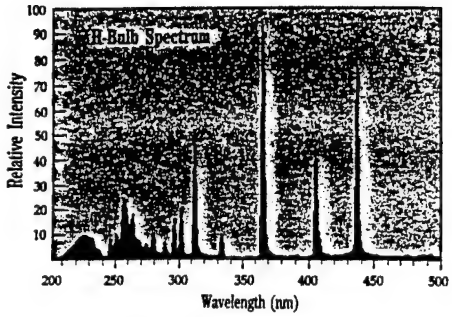

mercury filled

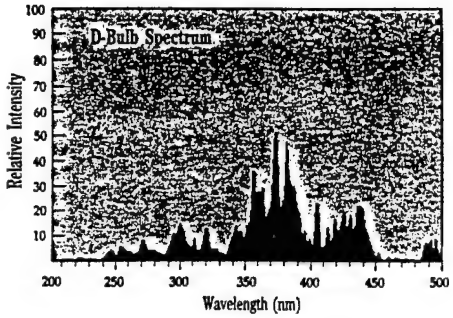

mercury mixture

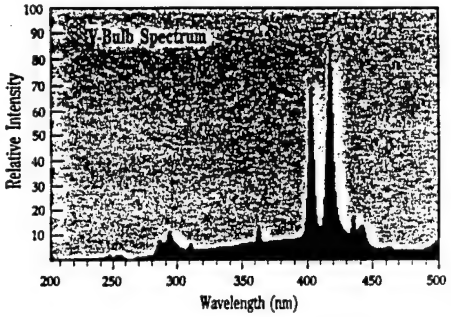

mercury mixture

Specifications: EPIQ 6000: Model F600

EPIQ 6000 Irradiator Model I600

Lamp Power:
- Full power: 600 w/inch (240 w/cm); 6000 watts total.
- Low power: 400 w/inch (160 w/cm); 4000 watts total.

Dimensions: 17.25" (43.8 cm) high x 8.14" (20.8 cm) wide x 10. 5" (26. 7 cm) long.

Weight: 30 lbs. (14 kg).

Cooling: 300 cfm (8.5 m^3/min) of filtered air at 6.4" to 8.0" (1.6 KPa to 2.0 KPa) water static pressure inside irradiator case.

Reflector Geometry: Elliptical. Focus 2.1" (53 mm) from irradiator face.

Substrate Location: 2.1" (53 mm) from irradiator face.

Mounting Position: Any angle.

Light Shield: Available upon request to customer specifications.

EPIQ 6000 Power Supply Model P600

Dimensions: 8.71" (22.1 cm) high x 18.38" (46.7 cm) wide x 29.67" (75.4 cm) long.

Rear Clearance: 12" (30.5 cm) required.

Weight: 190 lbs. (86 kg).

Power Levels:
- Full power: 6000 watts.
- Low power: 4000 watts.

Interconnecting Cables: Circular connectors with locking rings, not interchangeable with other Fusion power supply cables.

Voltage: 380, 415, 440 volts, three phase at 50 Hz. 380, 460, 480 volts, three phase, at 60 Hz.

(Operation from 200, 208, 220, or 240 volt requires customer supplied step-up transformer(s).)

Footprint: Same as previous 10-inch (25.4 cm) Fusion System irradiator.

Control Voltage: Supplied internally.

We reserve the right to incorporate changes and improvements without notice.

Fusion UV Curing
Fusion Systems Corporation®

Fusion UV Curing Systems™
7600 Standish Place
Rockville, Maryland 20855-2798 USA
(301) 251-0300 • FAX: (301) 279-0661

Fusion Japan K.K.
Tokyo, Japan
81 (0)3 3663-4580 • FAX: 81 (0)3 3663-3326

West Coast Region
Torrance, California
(310) 370-9920 • FAX: (310) 370-9152

Fusion Europe Ltd.
Alton, England
44-(0)420-544-516 • FAX: 44-(0)420-544-138

Midwest Region
Buffalo Grove, Illinois
(708) 459-9434 • FAX: (708) 459-4977

9/92 10M Printed in USA

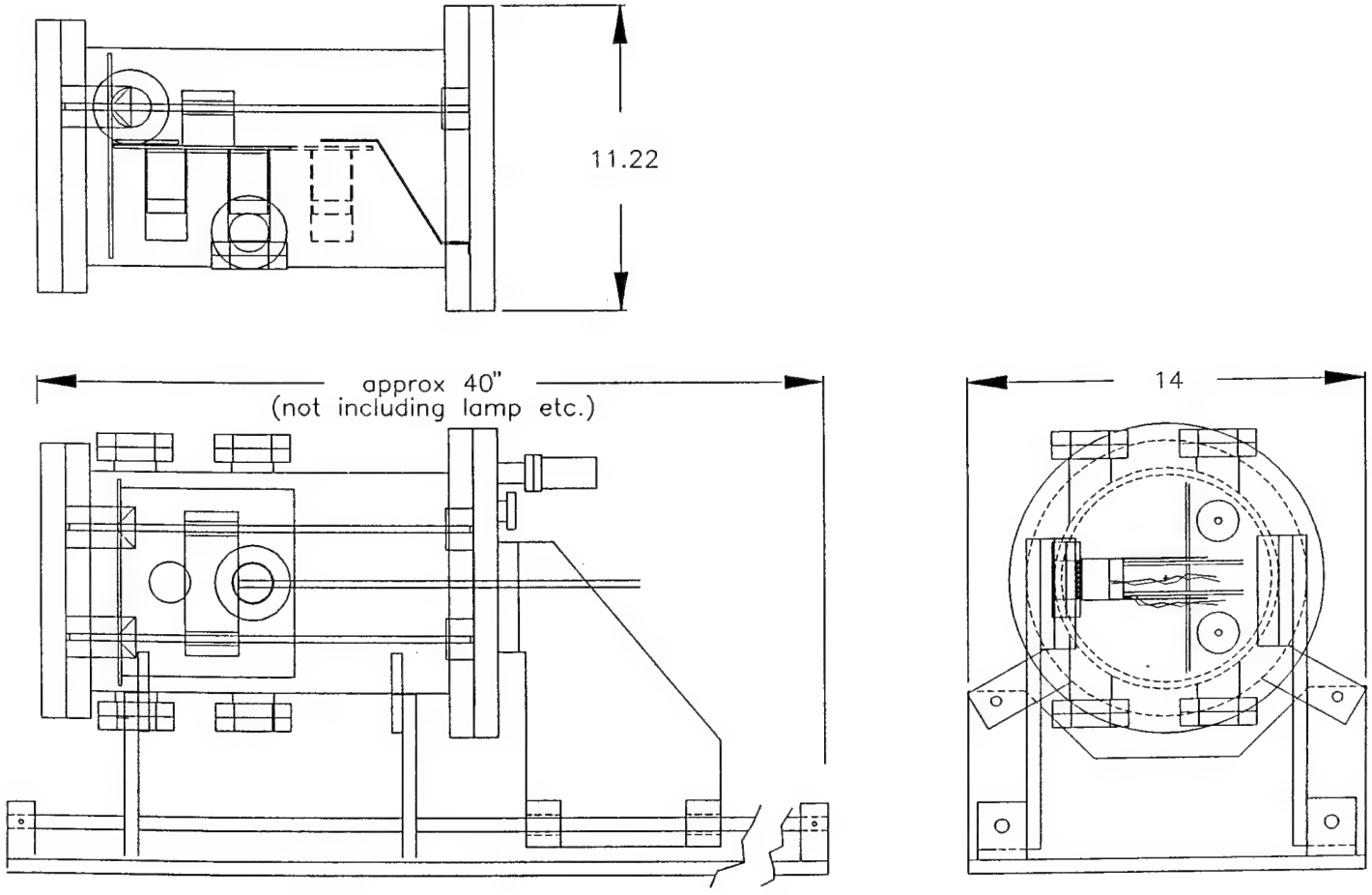

Figure 1 : Linear design of calibration apparatus

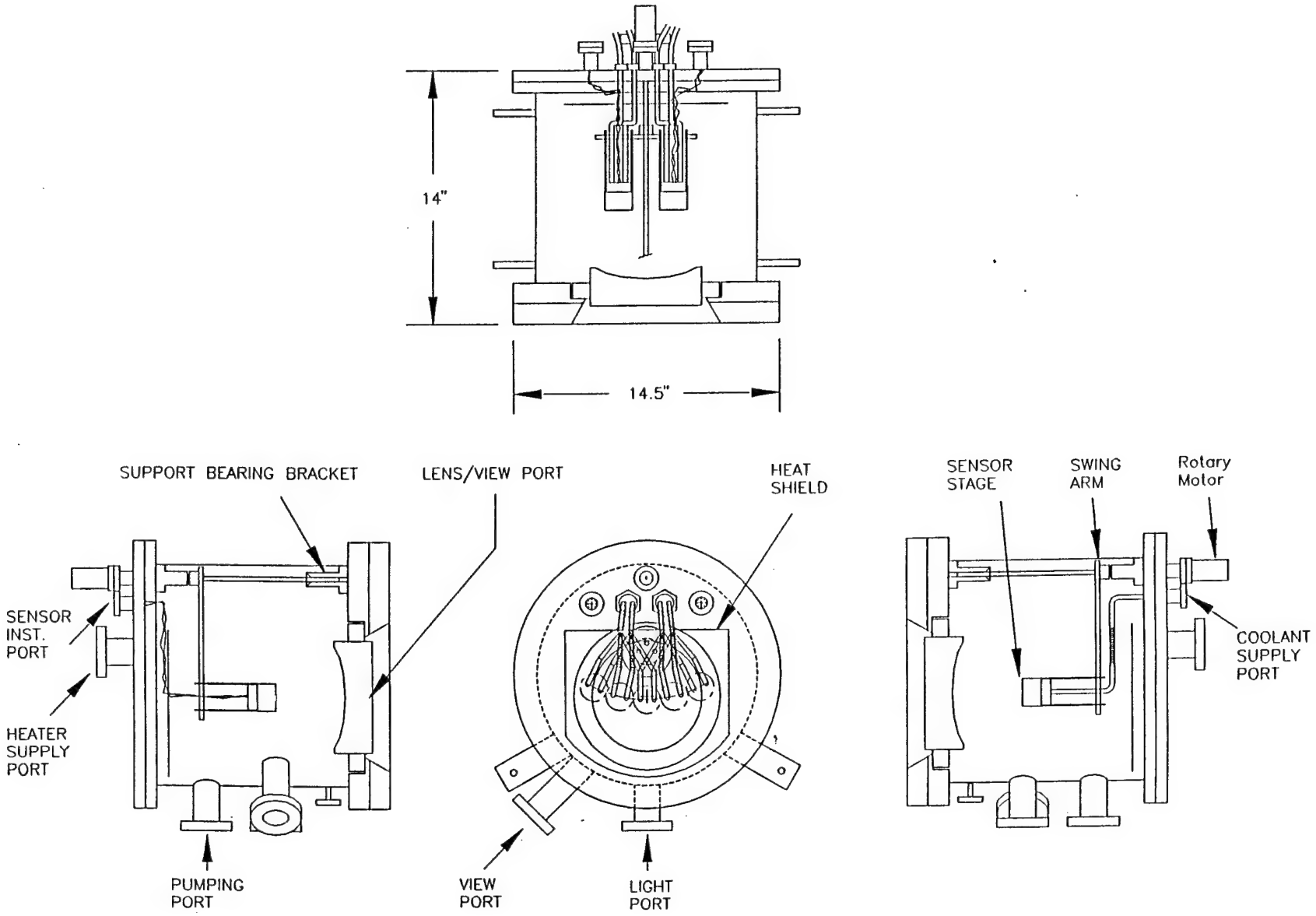

Figure 2 : Assembly of vacuum chamber, rotary system

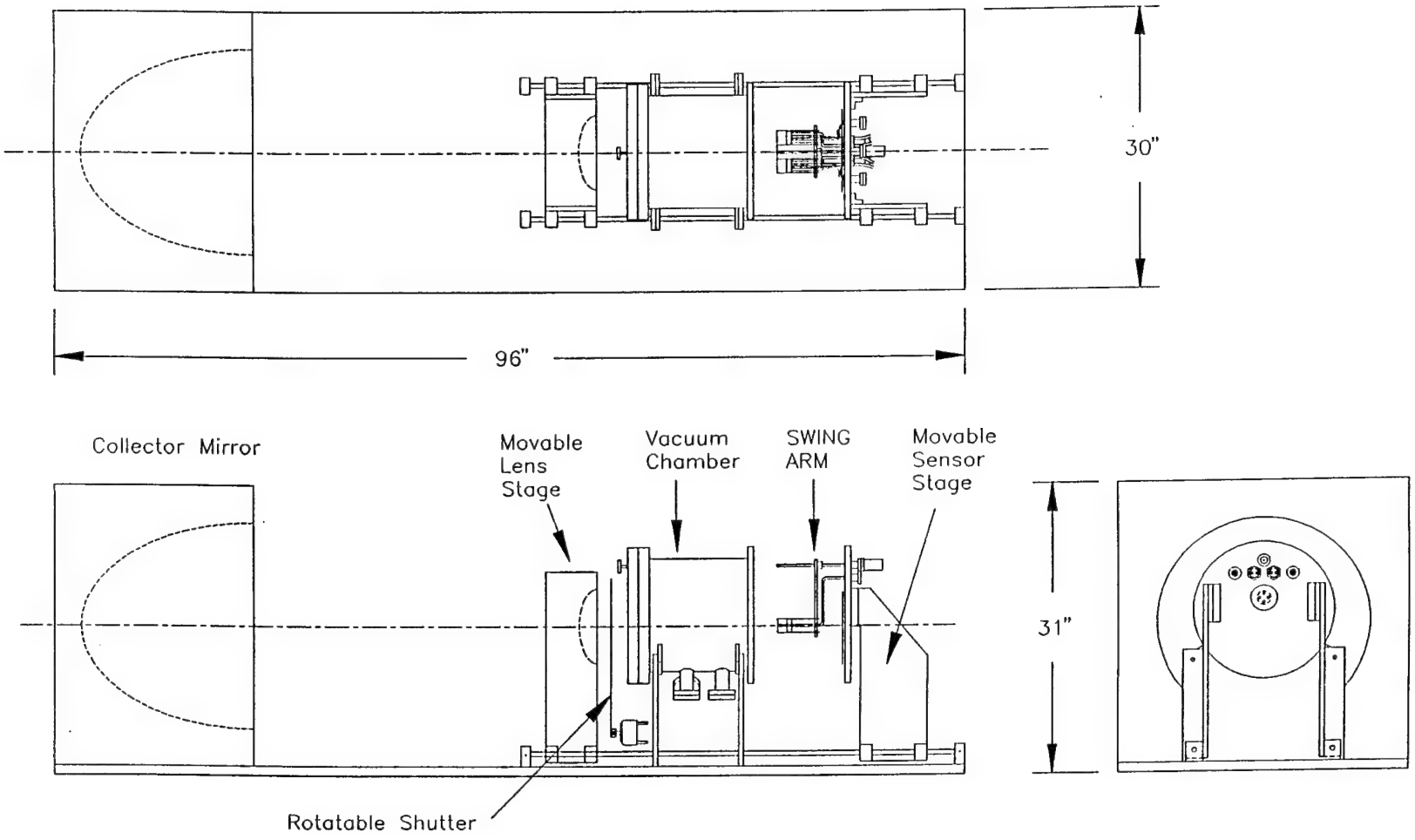

Figure 3 : Rotary design of calibration apparatus

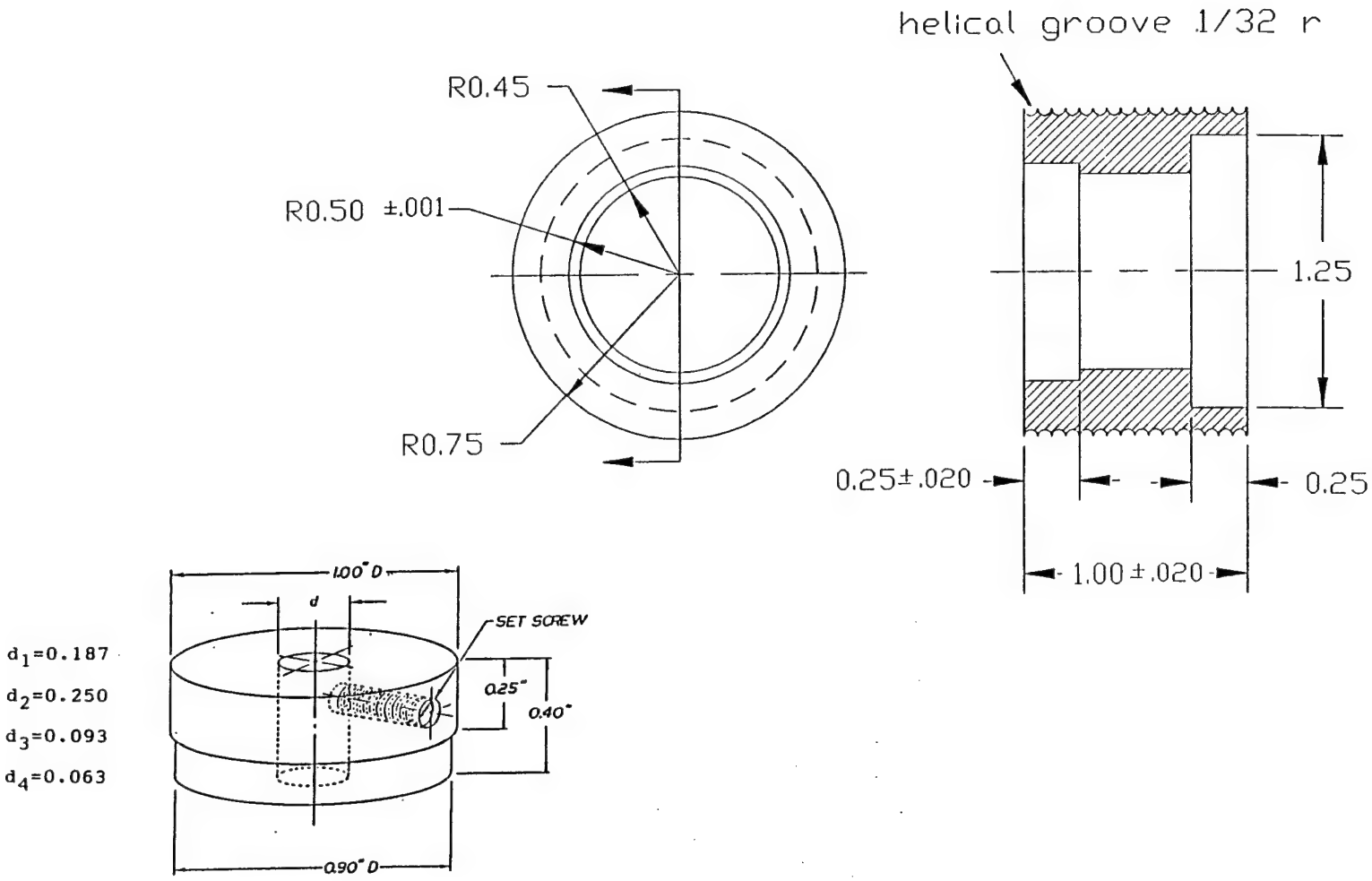

Figure 4 : Boron nitride sleeve and universal plug

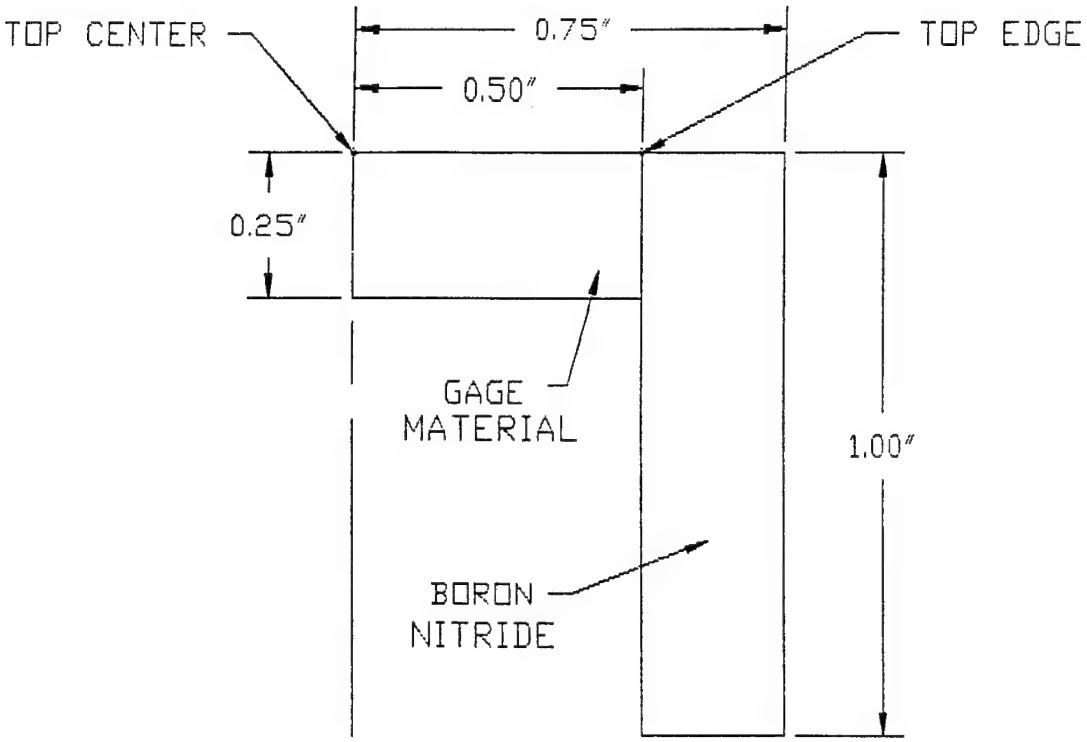

Axisymmetric cross-section of Boron Nitride sleeve and gage material plug

Figure 5 : Finite element model for heater stage

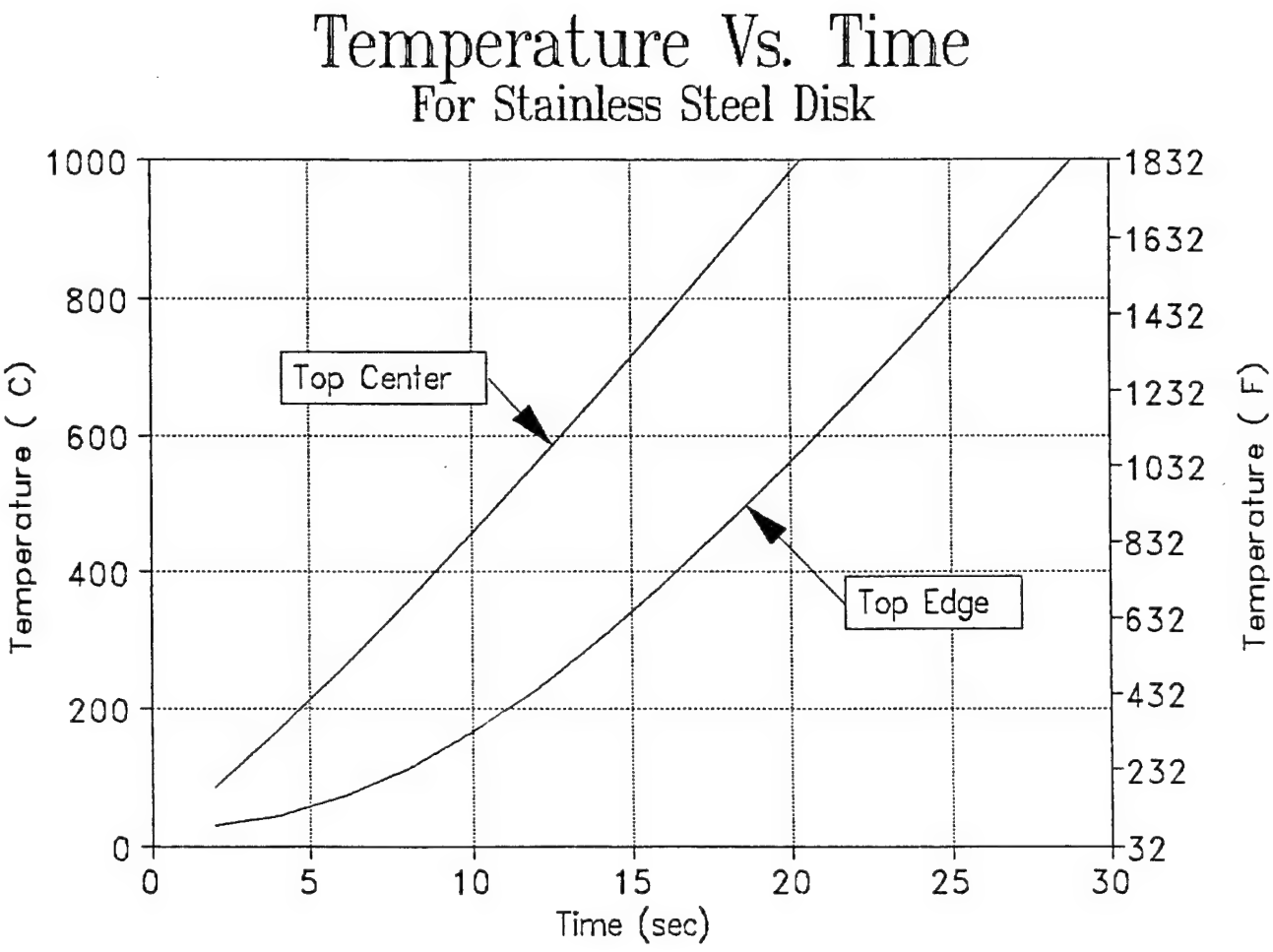

Figure 6 : Temperature response for S.S. at 1136 W/cm^2

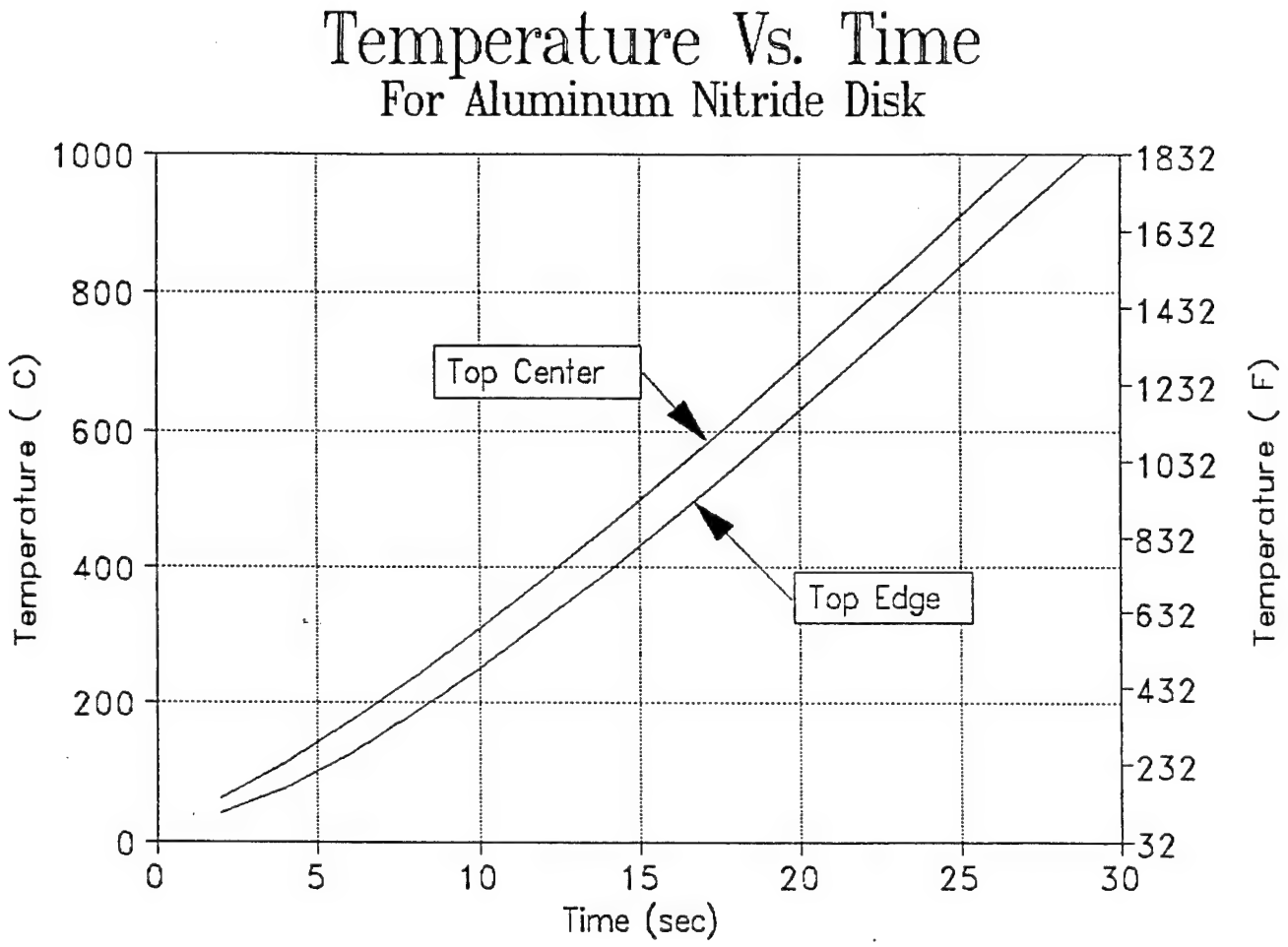

Figure 7 : Temperature response for AlN at 1136 W/cm^2

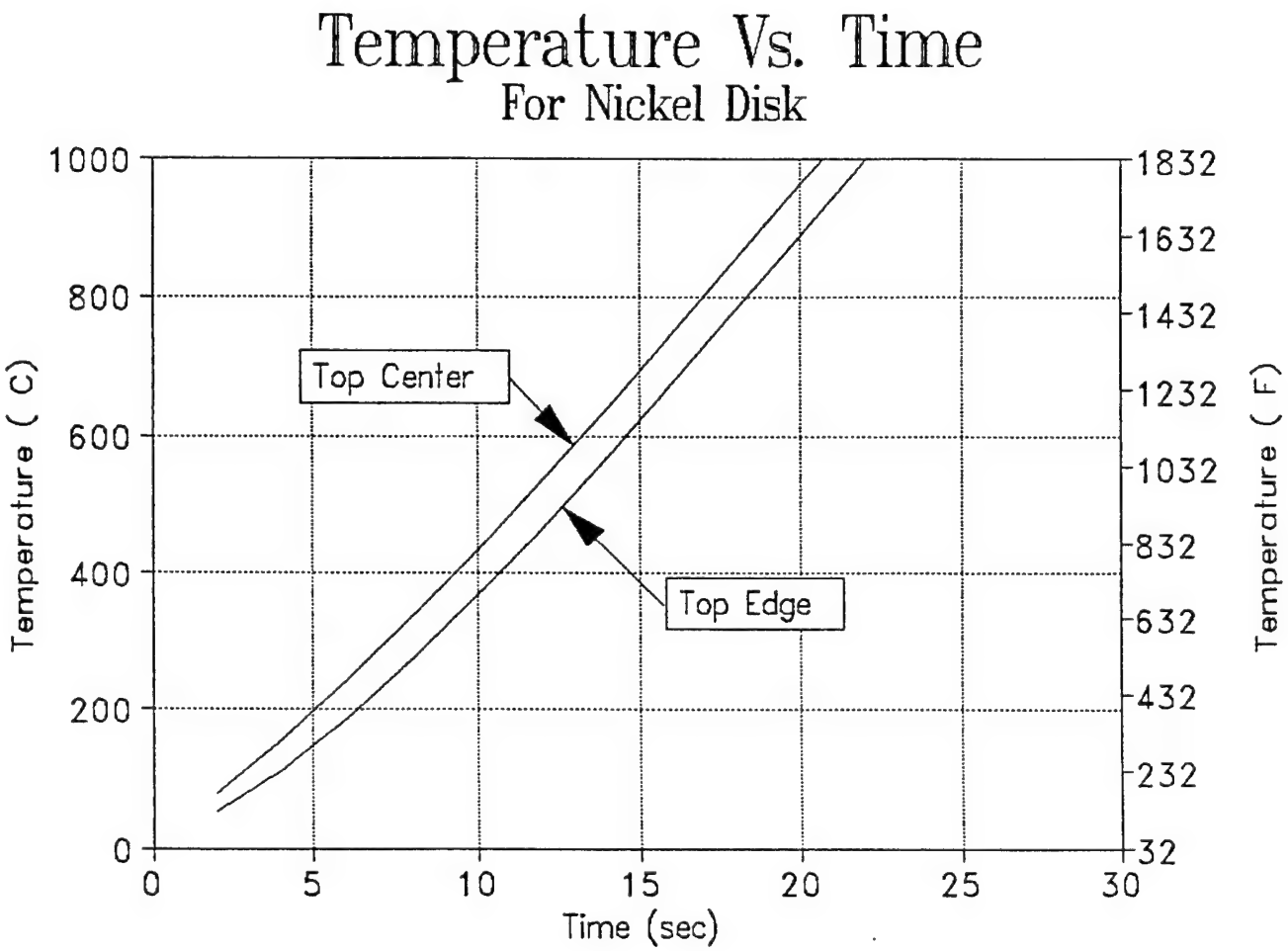

Figure 8 : Temperature response for Ni at 1136 W/cm^2

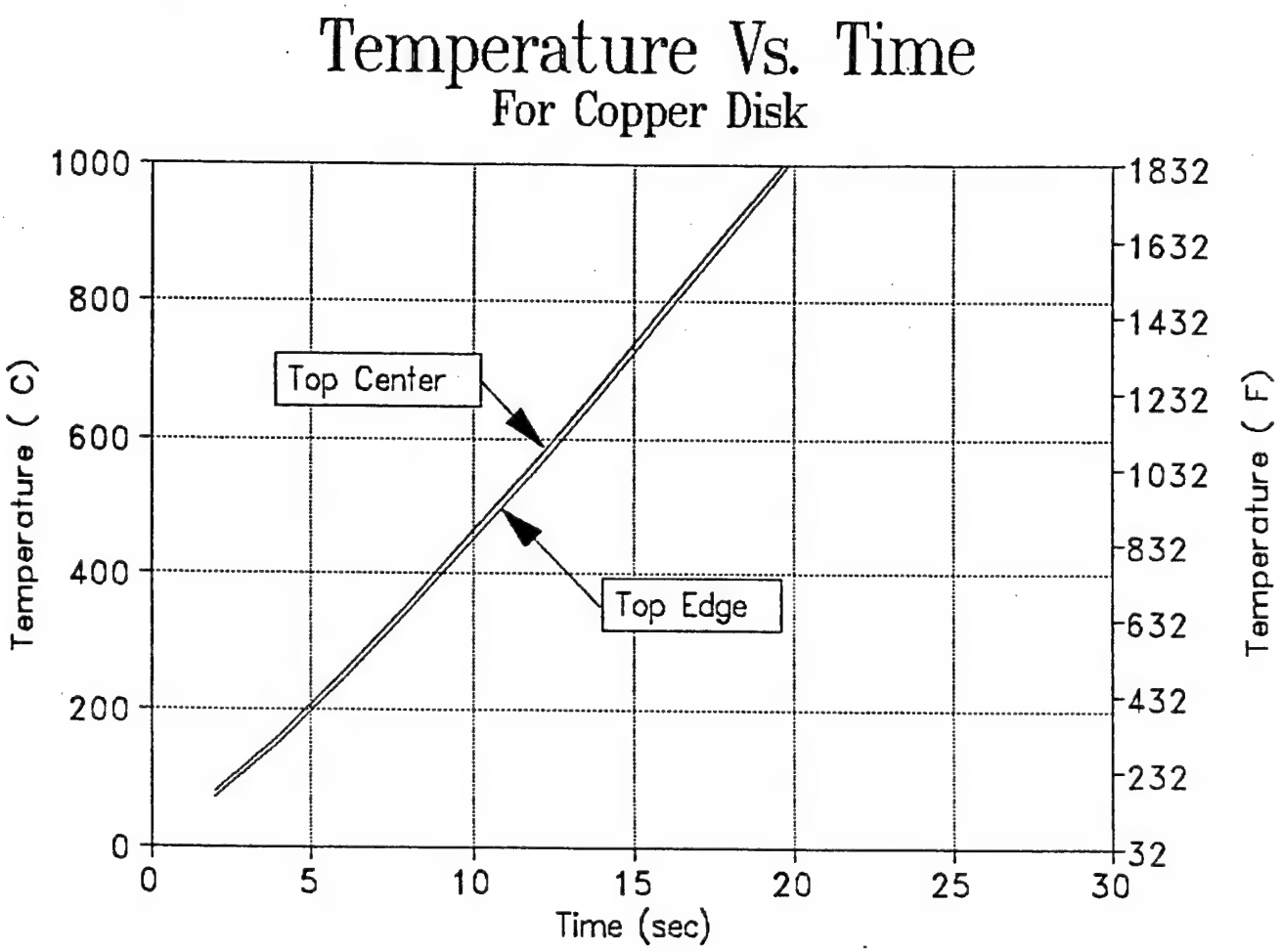

Figure 9 : Temperature response for Cu at 1136 W/cm^2

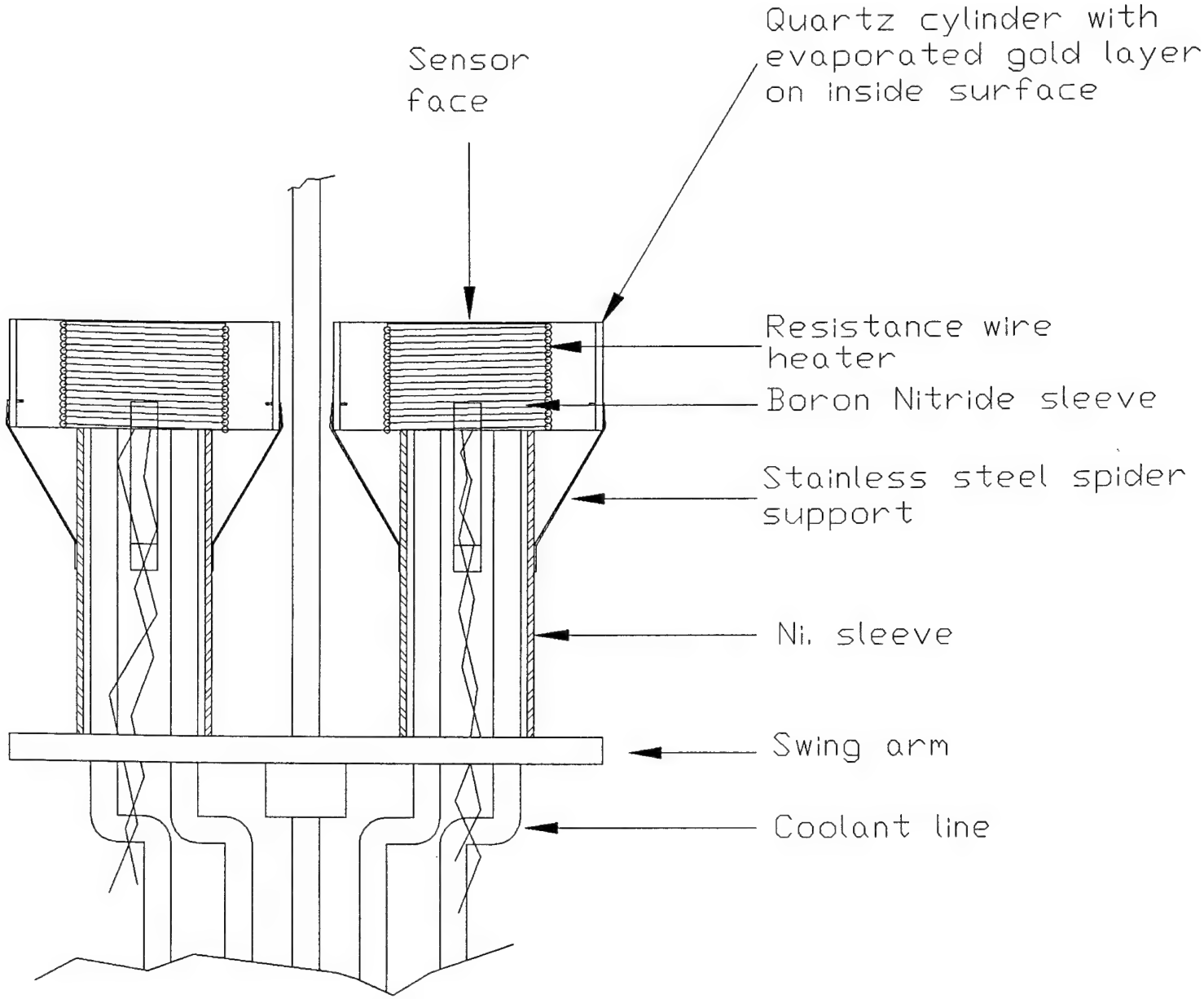

Figure 10 : Sensor stages mounted on swing-arm

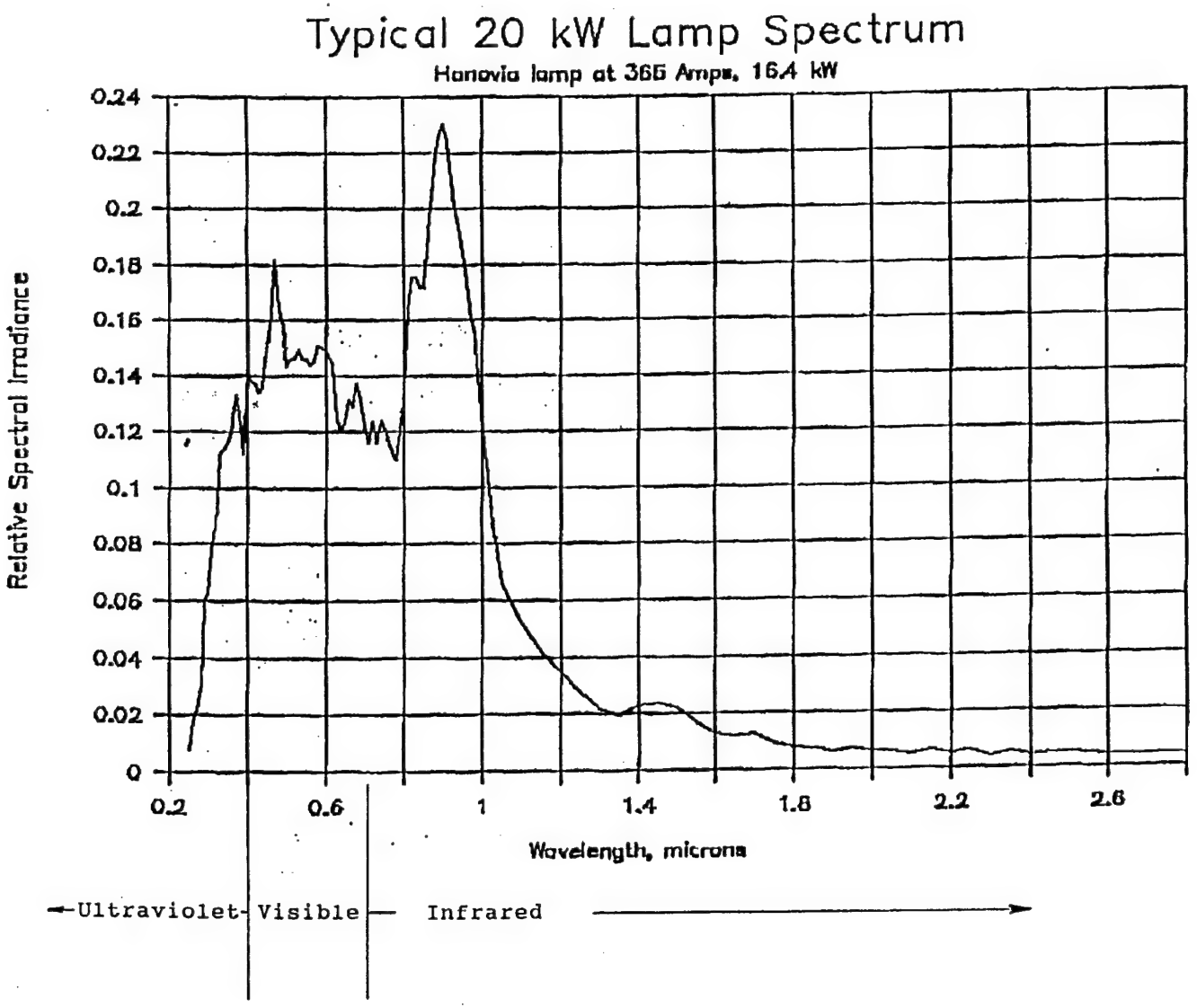

Figure 11 : Typical 20 kW lamp spectrum

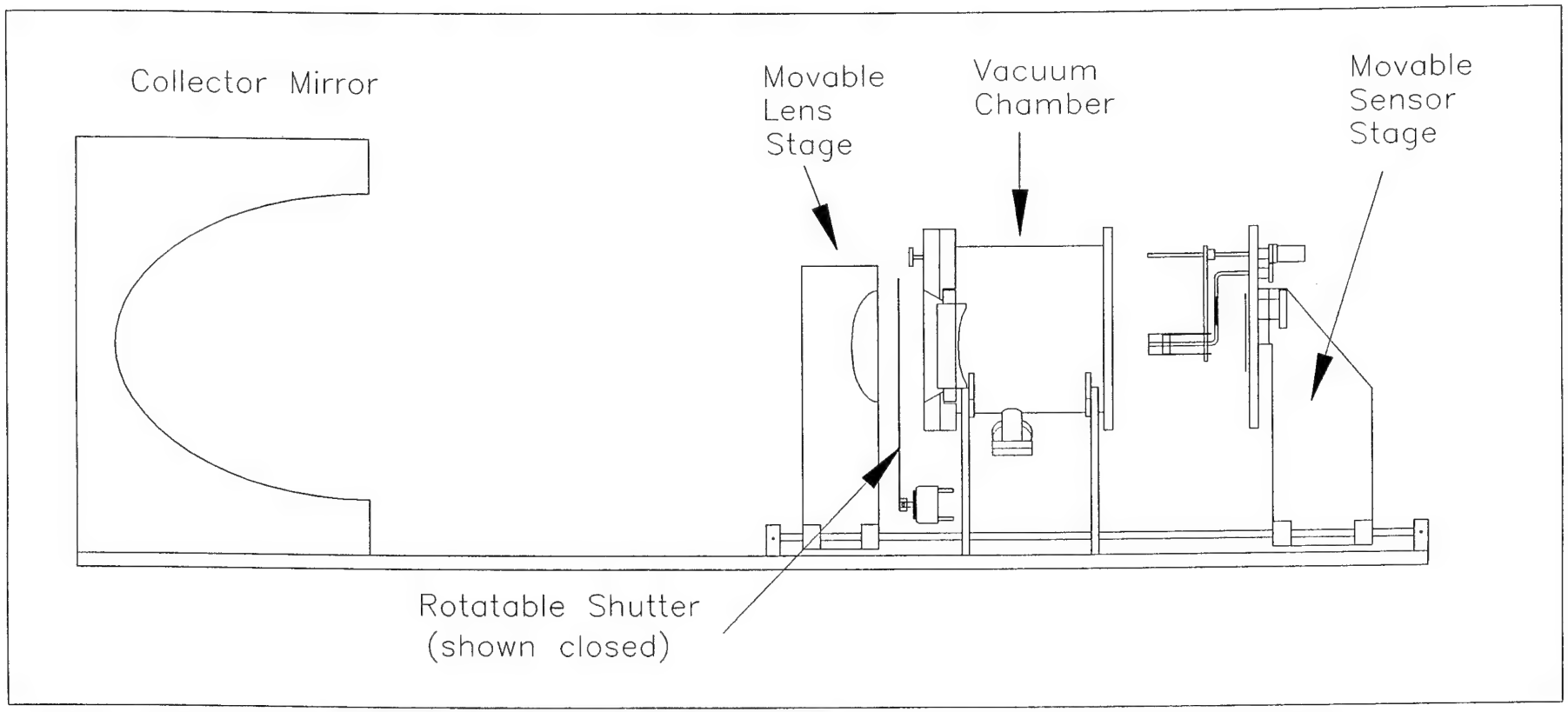

Figure 12 : Source and lenses configured for apparatus

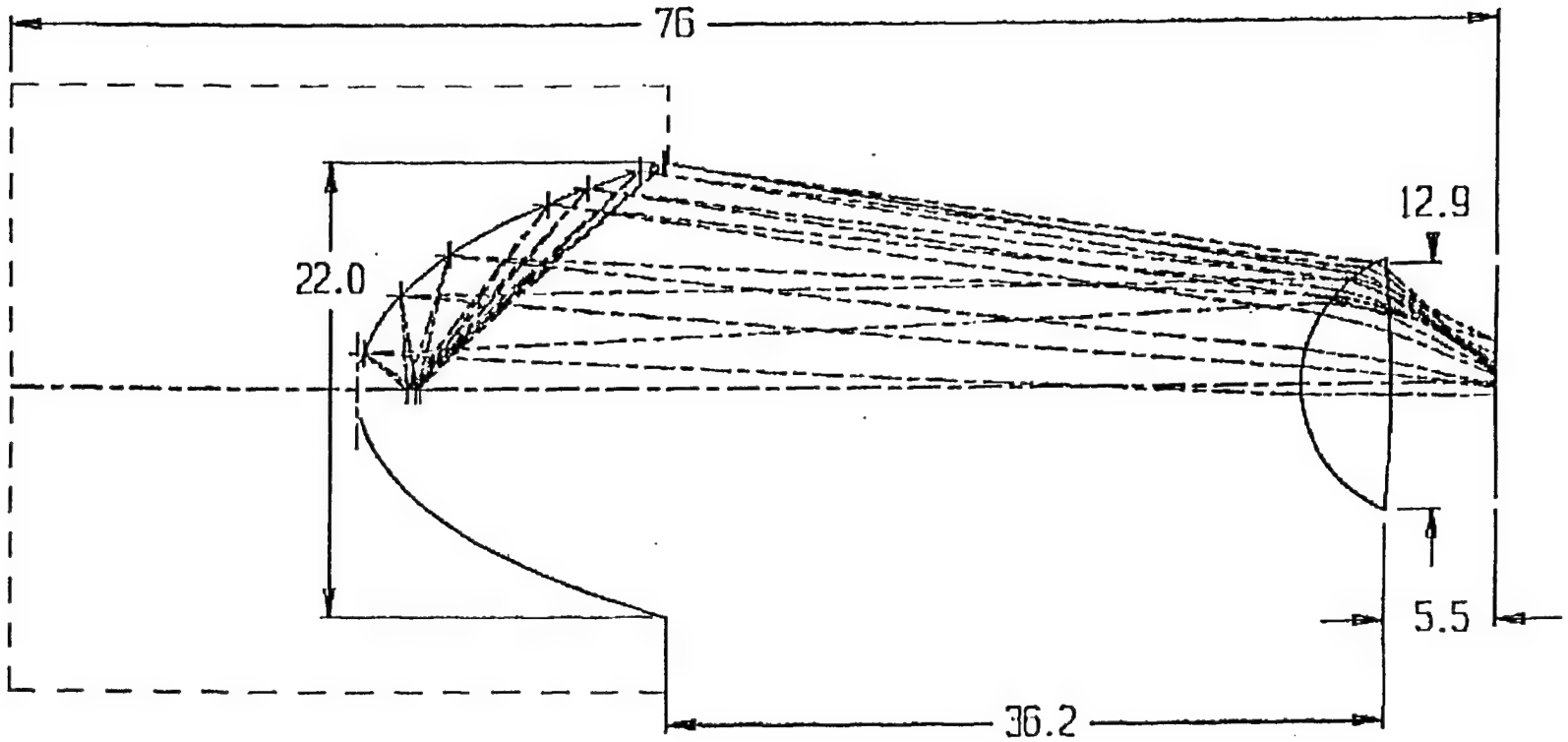

Figure 13 : Ray trace for anode and cathode in arc lamp source

CALIBRATION PROCEDURE

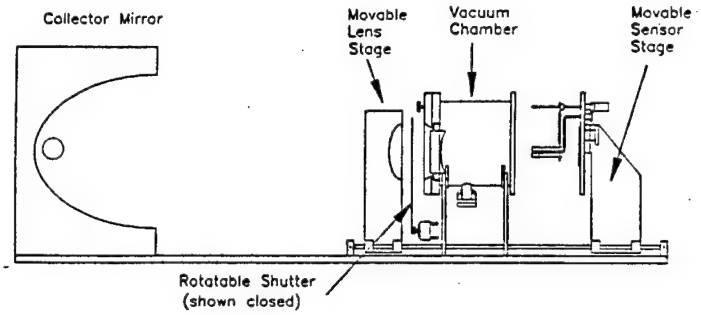

1. The chamber is open, the standard and sensor are installed.

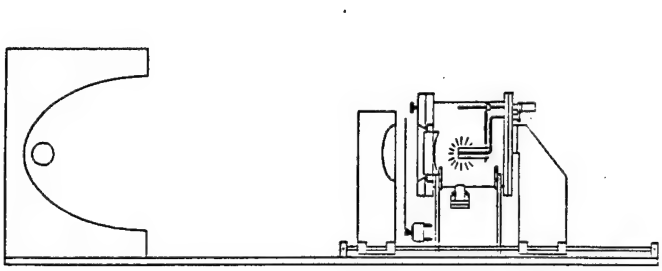

2. The chamber is closed, the pump is turned on, and the standard is heated to a low temperature.

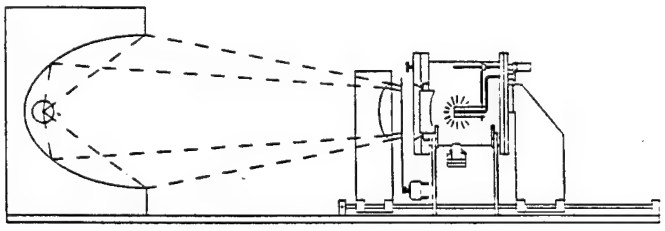

3. The lamp is turned on to 10% power and the large shutter is opened.

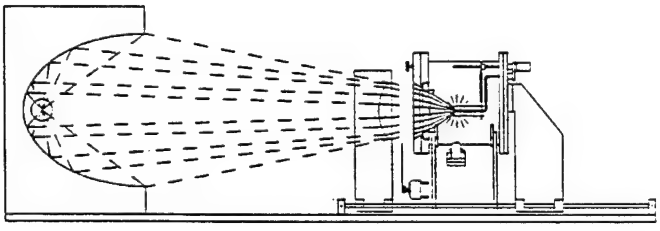

4. The lamp is at set power level, the small shutter is opened, and the standard is irradiated.

Figure 14 : Calibration procedure (steps 1 - 4)

CALIBRATION PROCEDURE (cont.)

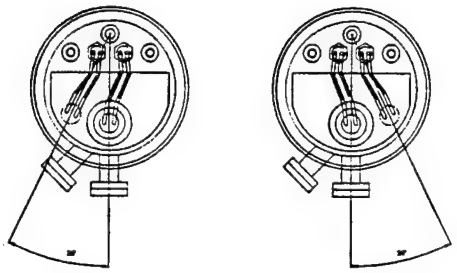

5. The stage is rotated and the sensor is placed in front of the lens.

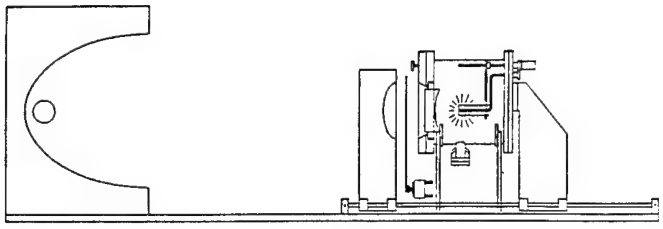

6. The sensor is heated to set-point.

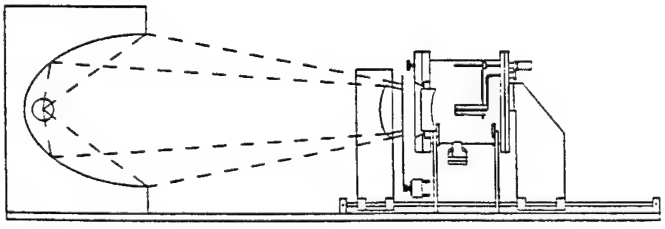

7. The lamp is turned on to 10% power and the large shutter is opened.

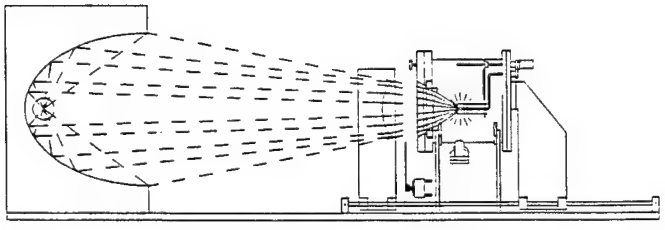

8. The lamp is at set power level, the small shutter is opened, and the sensor is irradiated.

Steps 6 through 8 are repeated for various temperature set-points at the same radiant power level. When the radiant power level is increased, steps 1 through 8 are repeated.

Figure 15 : (steps 5 - 8)

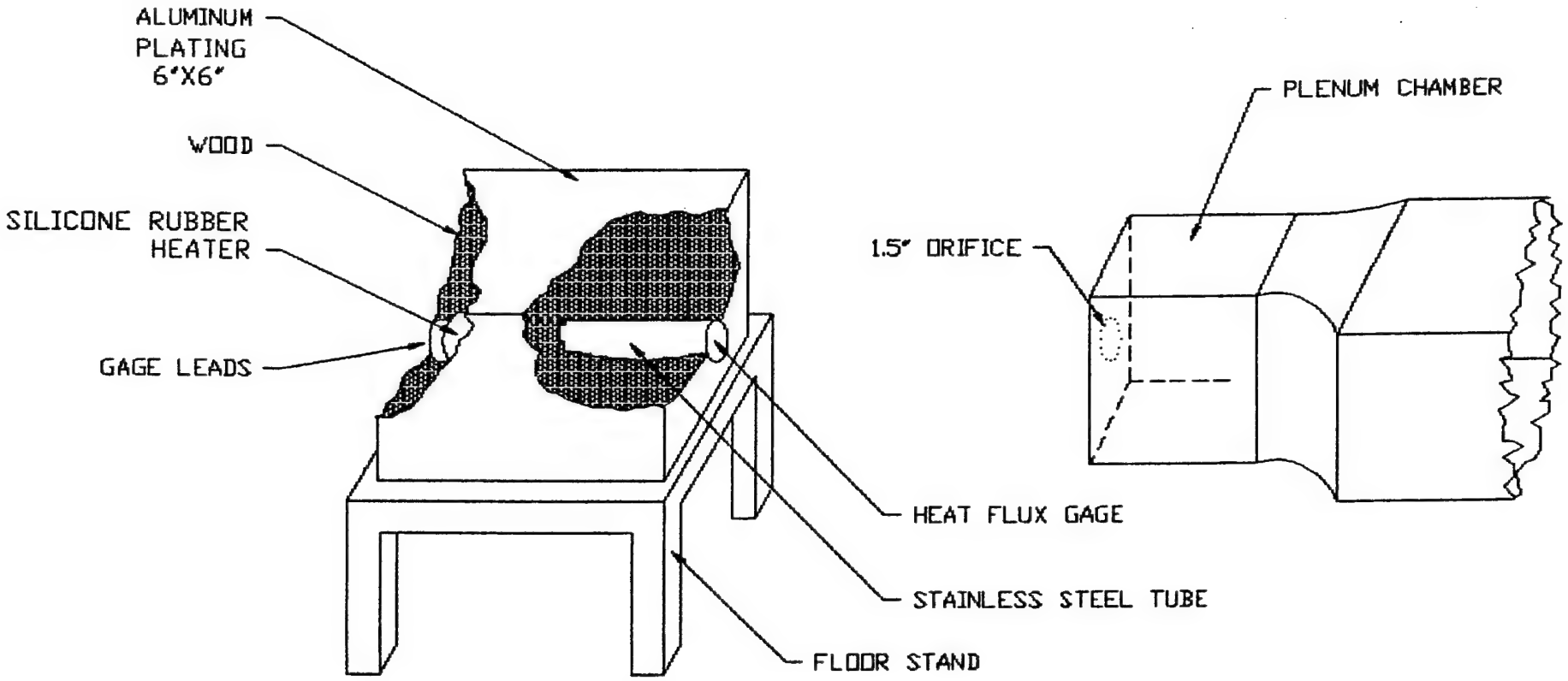

Figure 16 : Convection calibration apparatus - Virginia Tech

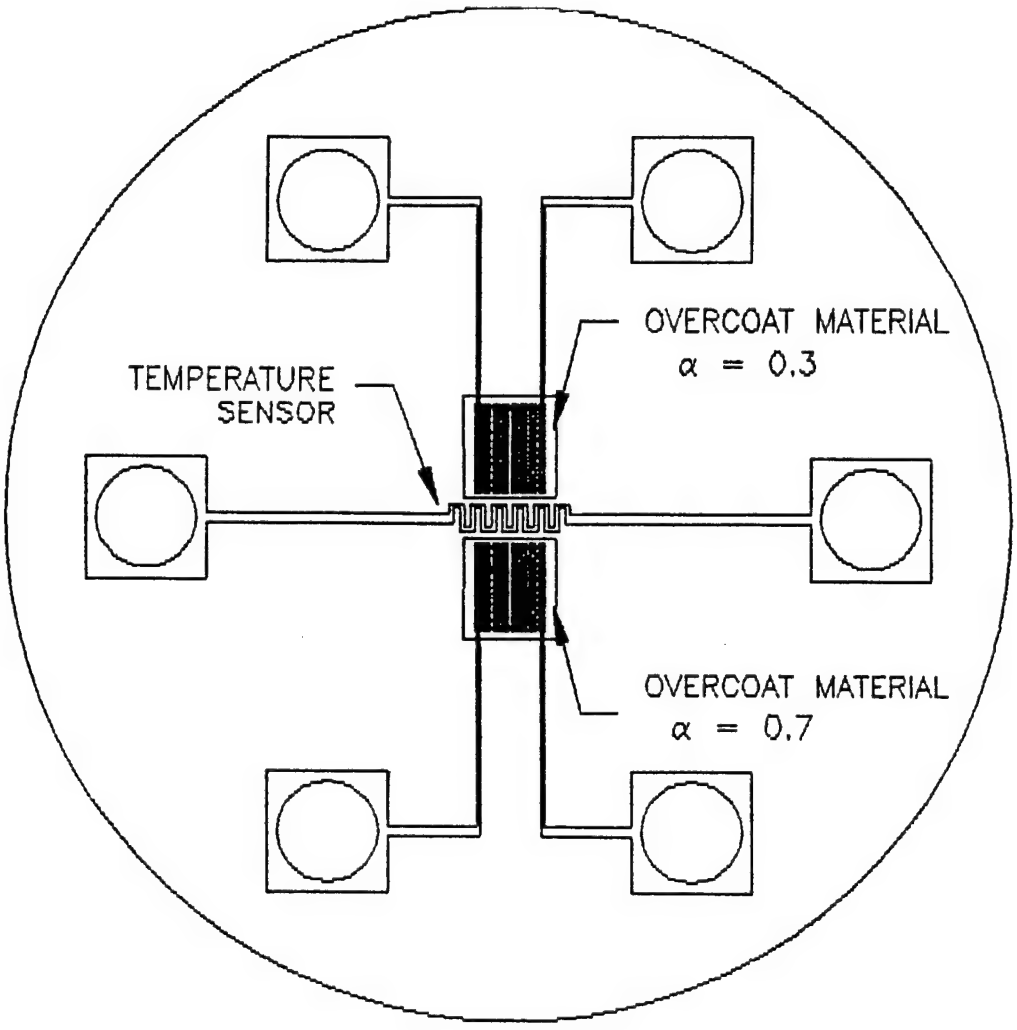

Figure 17 : Heat Flux Microsensor for separation method

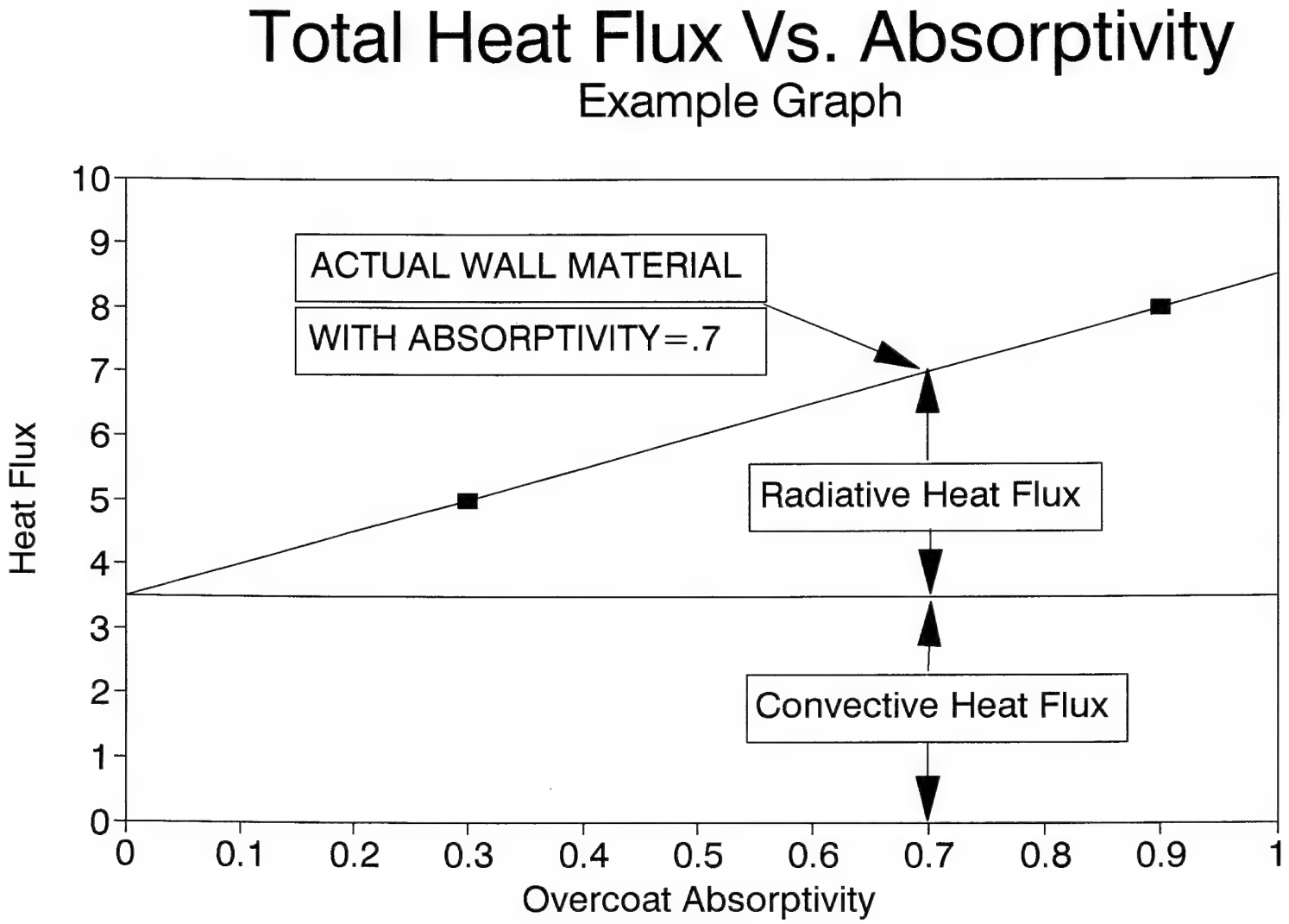

Figure 18 : Example graph of separation method

Test Set-up for Separation of Convective and Radiative Heat Flux

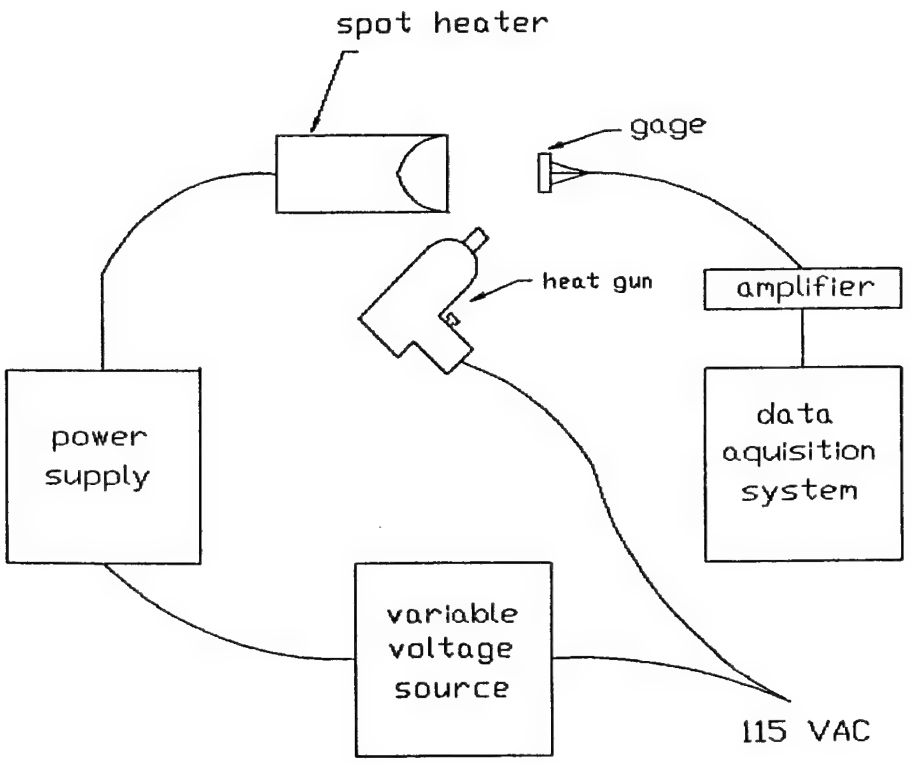

Figure 19 : Proposed test set-up for separation method

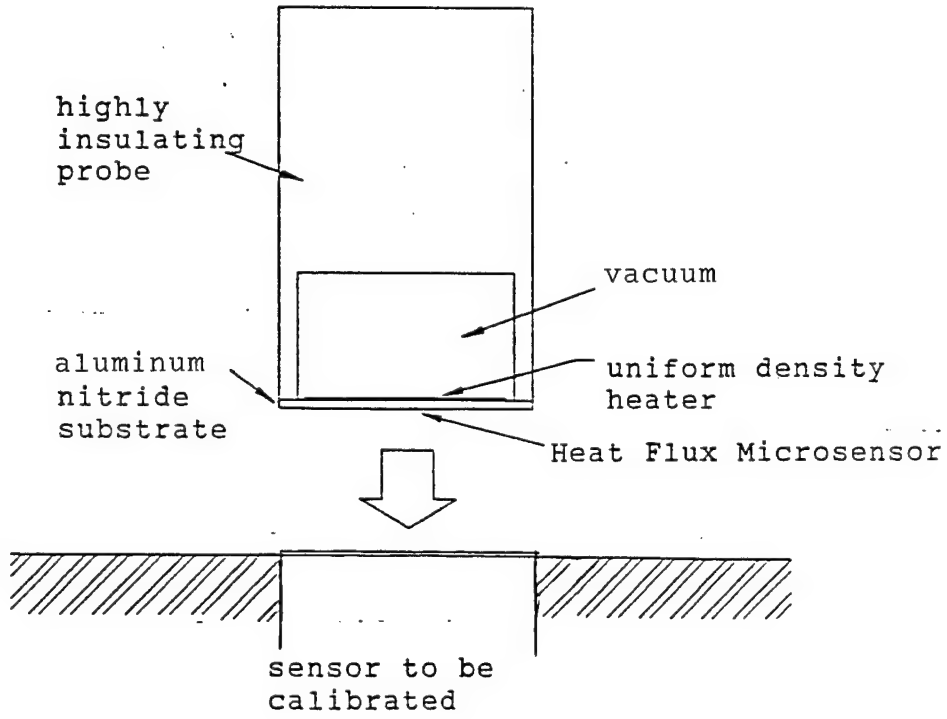

Figure 20 : Controlled Heat Flux Source (CHFS)

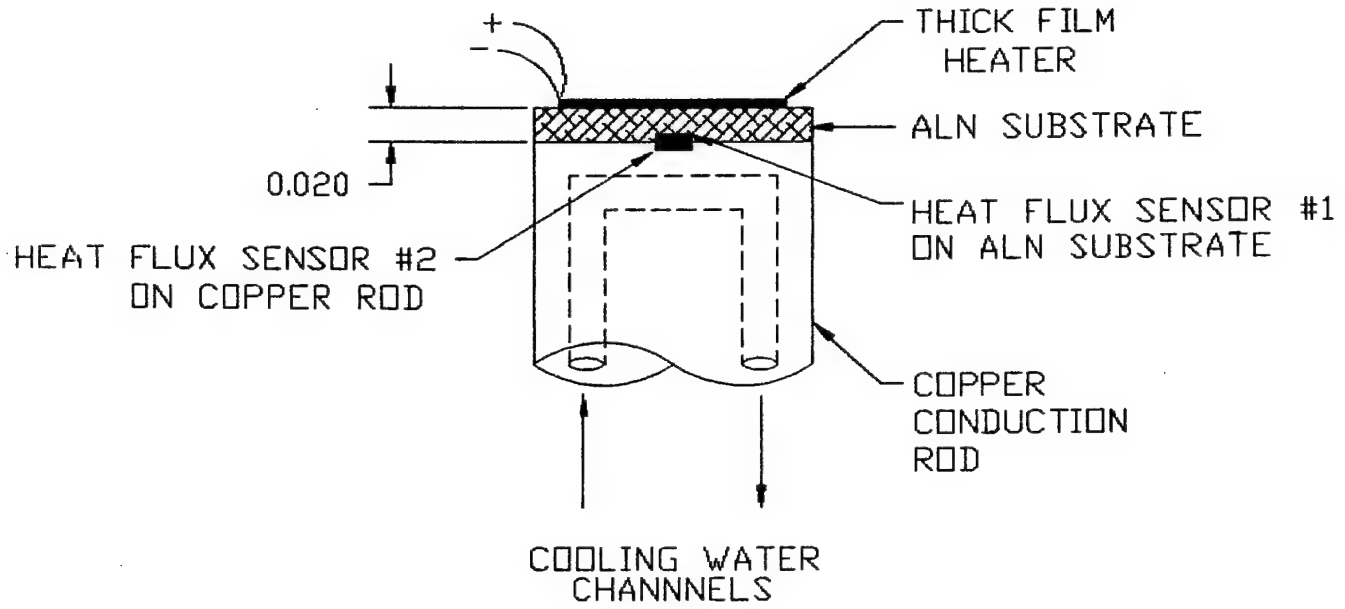

Figure 21 : Standardization method schematic

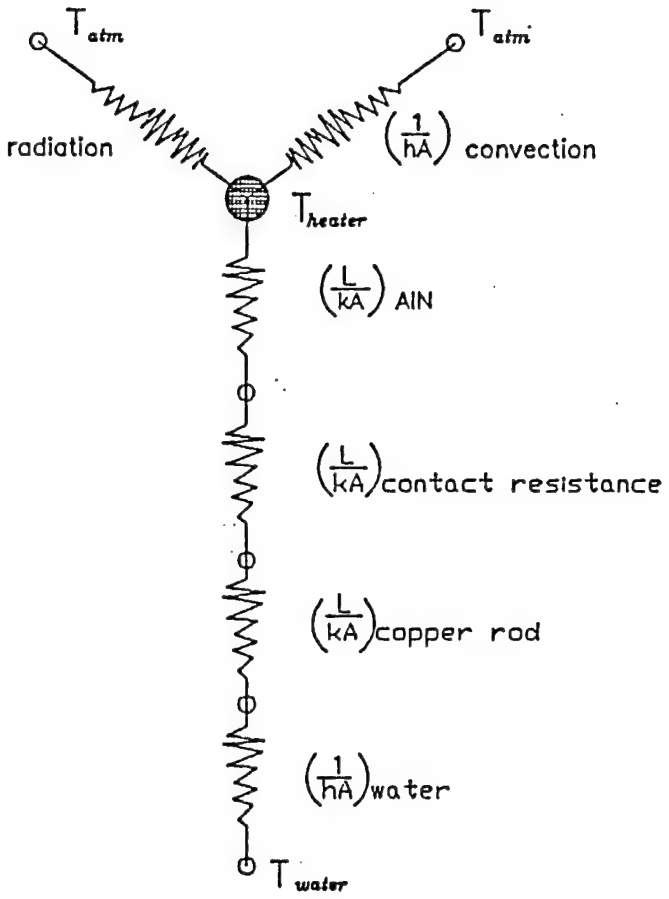

Figure 22 : Thermal circuit equivalent for standardization method

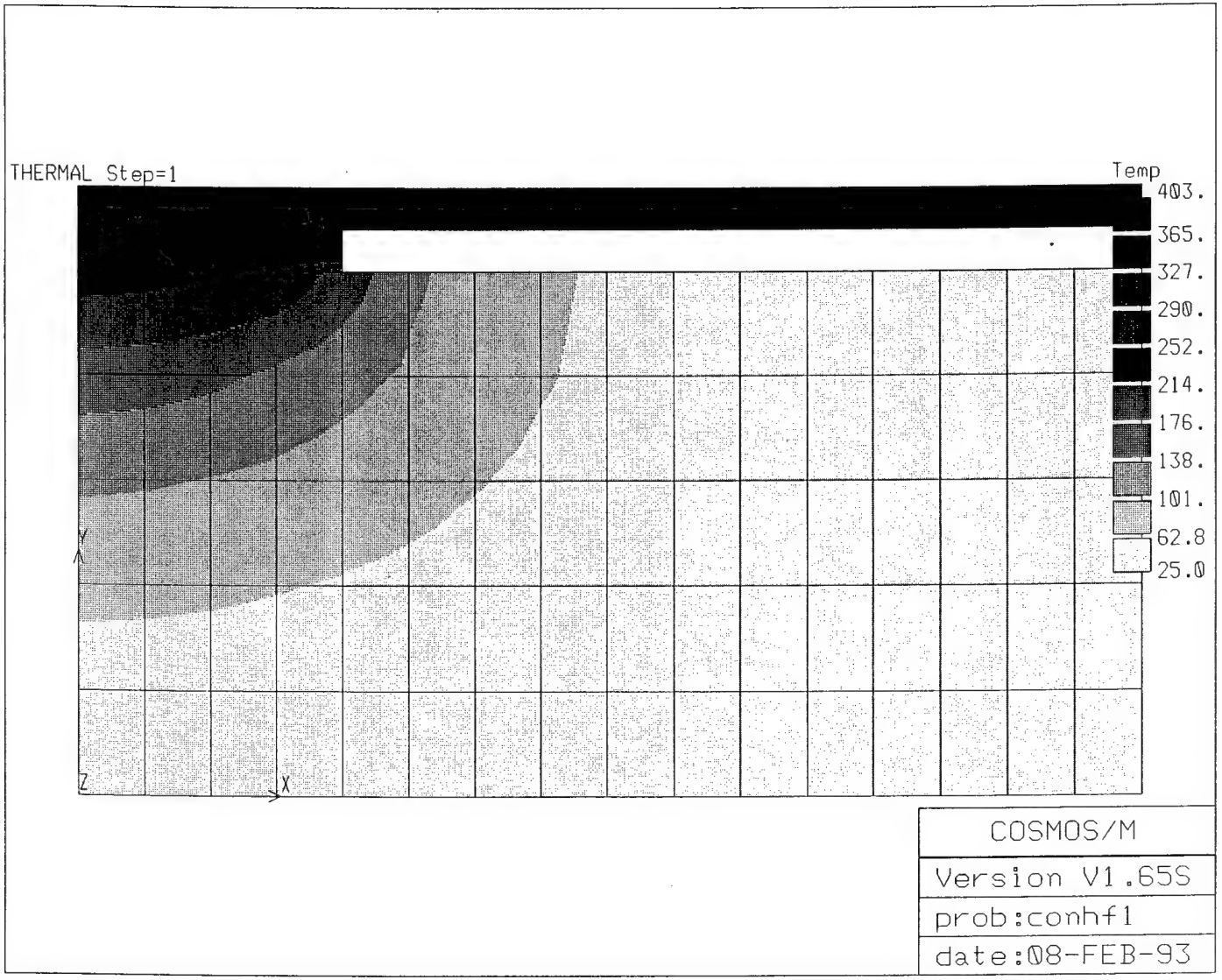

Figure 23 : Heat flux concentration - configuration 1

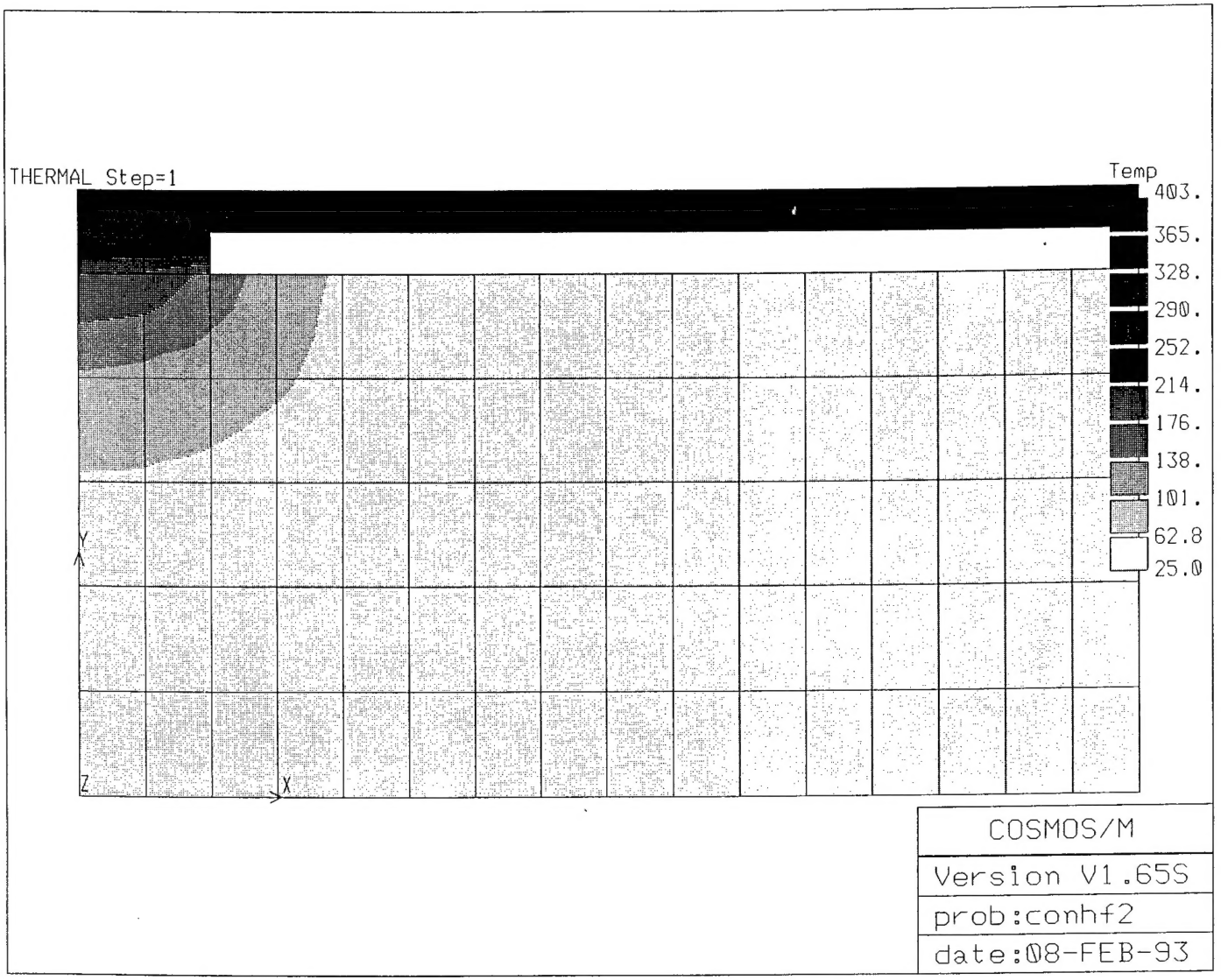

Figure 24 : Heat flux concentration - configuration 2

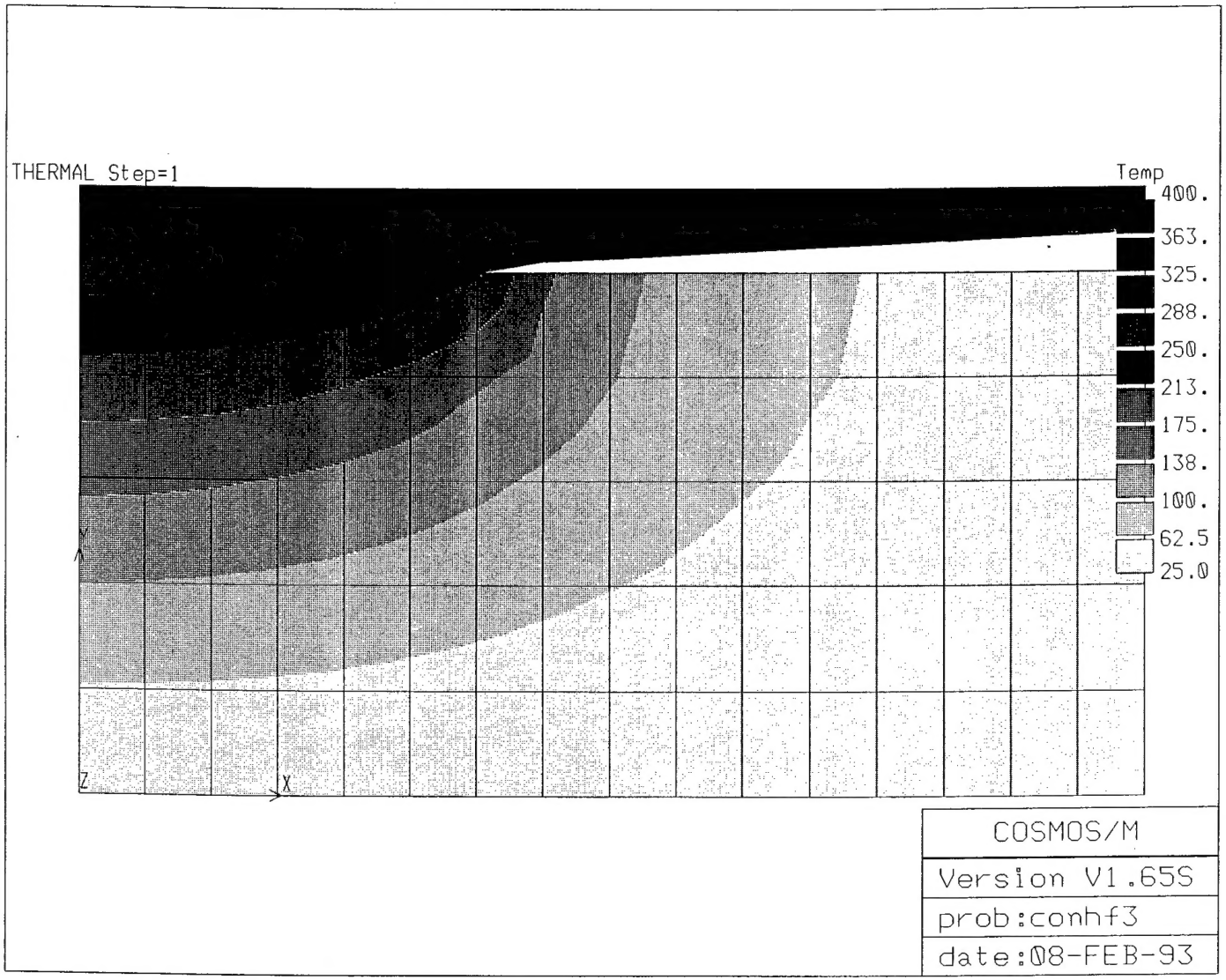

Figure 25 : Heat flux concentration - configuration 3

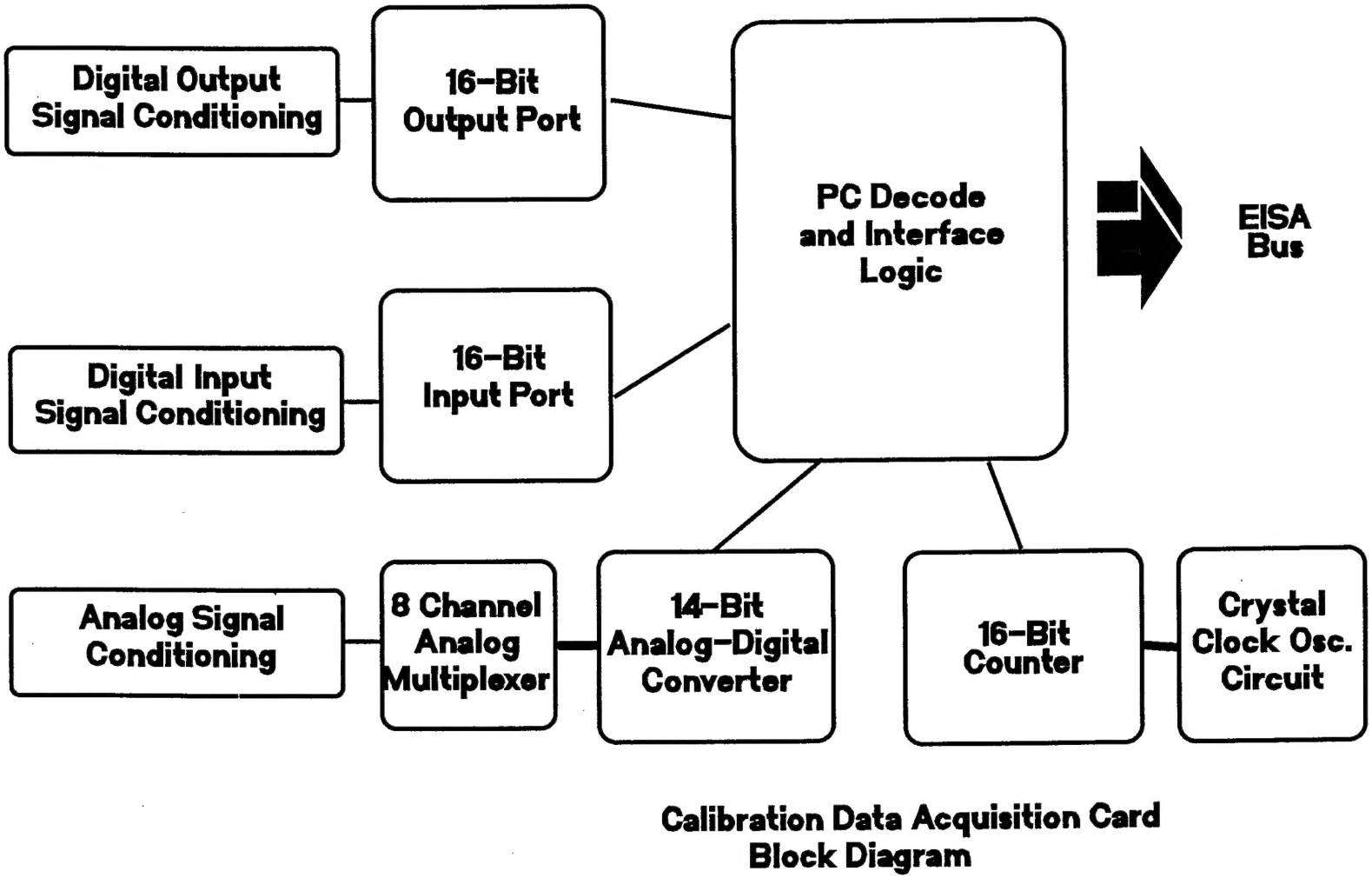

Figure 26 : Block diagram of calibration data acquisition card

AEDC Phase II System Process Diagram

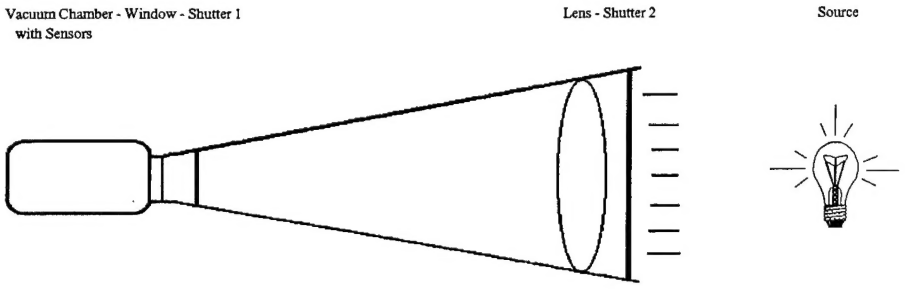

Source on, both shutters closed

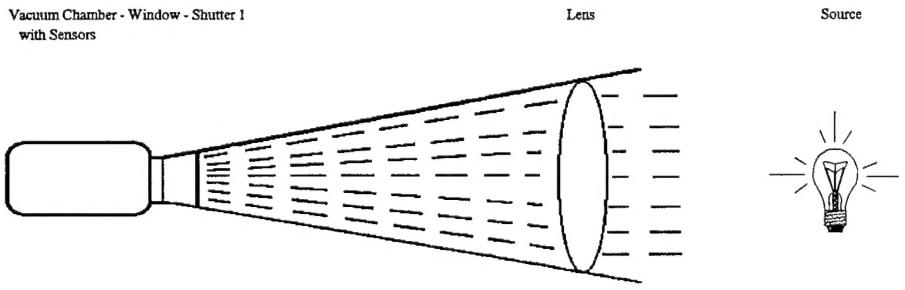

Source on, shutter 2 open, shutter 1 closed

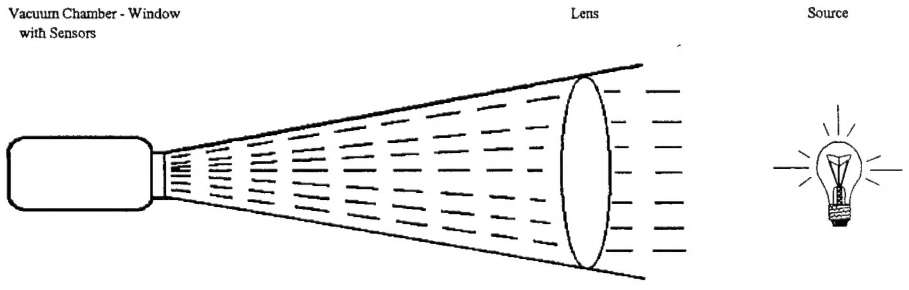

Source on both shutters open

Figure 27 : Shutter process diagram